JCI insight

Nucleolin promotes angiogenesis and endothelial metabolism along the onco-fetal axis in the human brain vasculature

Marc Schwab, … , Katrien De Bock, Thomas Wälchli

JCI Insight. 2023. https://doi.org/10.1172/jci.insight.143071.

Research In-Press Preview Angiogenesis Neuroscience

Graphical abstract

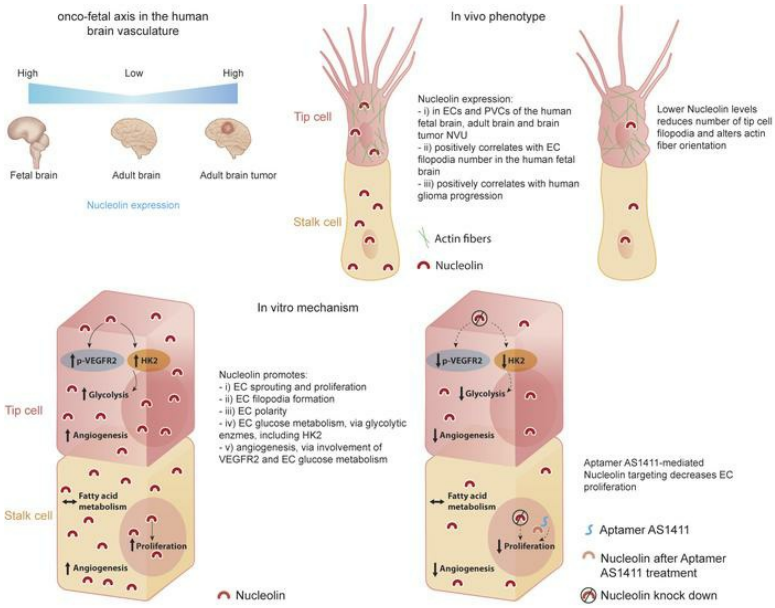

Find the latest version:

https://jci.me/143071/pdf

Nucleolin promotes angiogenesis and endothelial metabolism along the onco-fetal axis in the human brain vasculature

Marc Schwab[1,2,3,4], Ignazio de Trizio[5,6], Moheb Ghobrial[1,2,3,4,7,#], Jau-Ye Shiu[8,9,#], Oguzkan Sürücü[2,10], Francesco Girolamo[5], Mariella Errede[5], Murat Yilmaz[2,11], Johannes Haybaeck[12,13], Alessandro Moiraghi[14], Philippe P. Monnier[15,16,17], Sean E. Lawler[18,19], Jeffrey Greenfield[20], Ivan Radovanovic[3,4], Karl Frei[2], Ralph Schlapbach[21], Viola Vogel[7], Daniela Virgintino[5], Katrien De Bock[7], Thomas Wälchli[1,2,3,4*]

[1]Group of CNS Angiogenesis and Neurovascular Link, and Physician-Scientist Program, Institute for Regenerative Medicine, Neuroscience Center Zurich, and Division of Neurosurgery, University and University Hospital Zurich, Switzerland;[2]Division of Neurosurgery, University Hospital Zurich, Zurich, Switzerland; [3]Division of Experimental and Translational Neuroscience, Krembil Brain Institute, Krembil Research Institute, Toronto Western Hospital, University Health Network, University of Toronto, Toronto, Canada;[4]Division of Neurosurgery, Department of Surgery, Toronto Western Hospital, University Health Network, Toronto, Canada; [5]Department of Basic Medical Sciences, Neurosciences and Sense Organs, University of Bari School of Medicine, Bari, Italy; [6]Department of Neurosurgery, Neurocenter of Southern Switzerland, Regional Hospital Lugano, Lugano, Switzerland; [7]Laboratory of Exercise and Health, Institute of Exercise and Health, Department of Health Sciences and Technology; Swiss Federal Institute of Technology (ETH), Zurich, Switzerland; [8]Laboratory of Applied Mechanobiology, Department of Health Sciences and Technology, Swiss Federal Institute of Technology Zurich, Zurich, Switzerland; [9]Graduate Institute of Biomedical Sciences, China Medical University, Taichung 40402, Taiwan; [10]Center for Psychiatry Emmendingen, Emmendingen, Switzerland; [11]Department of Internal Medicine, Cantonal Hospital, Lucerne, Switzerland; [12]Department of Pathology, Neuropathology,

and Molecular Pathology, Medical University of Innsbruck, Innsbruck, Austria; [13] Diagnostic & Research Center for Molecular Biomedicine, Institute of Pathology, Medical University of Graz, Graz, Austria; [14]Division of Neurosurgery, Department of Clinical Neurosciences, University Hospital Geneva; Division of Neurosurgery, Department of Clinical Neurosciences, University Hospital Geneva; [15]Krembil Research Institute, Vision Division, Krembil Discovery Tower, Toronto, Ontario, Canada; [16]Department of Physiology, Faculty of Medicine, University of Toronto, Toronto, Ontario, Canada; [17]Department of Ophthalmology and Vision Sciences, Faculty of Medicine, University of Toronto, Ontario, Toronto, Canada; [18]Harvey Cushing Neuro-Oncology Laboratories, Department of Neurosurgery, Harvard Medical School and Brigham and Women's Hospital, Boston, MA, 02115, USA; [19]Department of Pathology and Laboratory Medicine, Legoretta Cancer Center, Brown University, Providence, RI, 02903, USA; [20]Department of Neurological Surgery, Weill Cornell Medical College, New York, New York; [21]Functional Genomics Center Zurich, ETH Zurich and University of Zurich, Zurich, Switzerland; [#]These authors contributed equally

Running title: Nucleolin is an onco-fetal protein expressed in human fetal brain development and reactivated in human glial brain tumors regulating angiogenesis and vascular metabolism

*Corresponding author:
Thomas Wälchli
Group of CNS Angiogenesis and Neurovascular link
Division of Neurosurgery
Neuroscience Center Zurich, and Division of Neurosurgery
University and University Hospital Zurich

Group of Brain Vasculature and Perivascular Niche
Division of Neurosurgery,
Krembil Neuroscience Institute

Toronto Western Hospital, University of Toronto

Frauenklinikstrasse 10
CH-8057 Zürich / CH-8091 Zurich, Switzerland
Phone : +41 44 635 32 16 / +41 79 243 86 10
Fax : +41 44 635 33 03
E-mail : waelchli@irem.uzh.ch
thomas.waelchli@usz.ch

60 Leonard Avenue
Toronto, Ontario, M5T 2S8
+1 647 394 86 10
thomas.waelchli@uhn.ca
thomas.waelchli@uoft.ca

ABSTRACT

Glioblastoma is amongst the deadliest human cancers and is highly vascularized. Angiogenesis is very dynamic during brain development, almost quiescent in the adult brain but reactivated in vascular-dependent CNS pathologies including brain tumors. The onco-fetal axis describes the reactivation of fetal programs in tumors, but its relevance in endothelial- and perivascular cells of the human brain vasculature in glial brain tumors is unexplored. Nucleolin is a regulator of cell proliferation and angiogenesis, but its roles in the brain vasculature remain unknown. Here, we studied the expression of Nucleolin in the neurovascular unit in human fetal brains, adult brains and human gliomas in vivo and its effects on sprouting angiogenesis and endothelial metabolism in vitro. Nucleolin is highly expressed in endothelial- and perivascular cells during brain development, downregulated in the adult brain, and upregulated in glioma. Moreover, Nucleolin expression correlated with glioma malignancy in vivo. In culture, siRNA-mediated Nucleolin knock-down reduced human brain endothelial cell (HCMEC) and human umbilical vein endothelial cell (HUVEC) sprouting angiogenesis, proliferation, filopodia extension, and glucose metabolism. Furthermore, inhibition of Nucleolin with the aptamer AS1411 decreased brain endothelial cell proliferation in vitro. Mechanistically, Nucleolin knock-down in HCMECs and HUVECs uncovered regulation of angiogenesis involving VEGFR2 and of endothelial glycolysis. These findings identify Nucleolin as a neurodevelopmental factor reactivated in glioma that promotes sprouting angiogenesis and endothelial metabolism, characterizing Nucleolin as an onco-fetal protein. Our findings have potential implications in the therapeutic targeting of glioma.

INTRODUCTION

Glioblastomas (GBMs) are amongst the deadliest human cancers, with a less than 15-month median survival and a 5-year survival of only 5% (1-3) (see Supplementary Introduction).

A typical feature of GBMs is their high grade of vascularization established by angiogenesis, the growth of new blood vessels (4-6). GBM growth is highly dependent on angiogenesis and mutual interaction among the cellular components of the neurovascular unit (NVU)/perivascular niche (PVN) including endothelial- and perivascular cells such as pericytes, astrocytes, neurons, macrophages, microglia, and neuronal stem cells (7). Accordingly, therapeutic approaches targeting angiogenesis and the NVU in GBM have been proposed (1, 8-10). However, despite promising preclinical data, anti-angiogenic agents have failed to show a survival benefit in randomized controlled trials in GBM patients (1, 8). This is mainly due to our limited knowledge about the cellular and molecular mechanisms regulating angiogenesis and the NVU in brain tumors (1, 4, 5, 7, 11, 12).

Whereas angiogenesis is highly dynamic during brain development, the brain vasculature is mostly quiescent in the adult brain with only few proliferating endothelial cells (ECs) ensuring a stable blood-brain barrier (BBB) (11, 13-16). Interestingly, angiogenesis and the NVU are reactivated in a variety of angiogenesis-dependent central nervous system (CNS) pathologies such as brain tumors, brain vascular malformations, or stroke (4, 7, 11, 14, 17). However, the molecular signaling cascades reactivated in brain tumors remain elusive. For instance, whether there is molecular similarity between developmental- and tumor angiogenesis (termed onco-fetal axis (18-25), and how neurodevelopmental pathways regulate brain tumor (vessel) growth remains poorly defined. Thus, in order to better understand pathological brain tumor vasculature, a molecular understanding of normal vascular brain development is crucial (11, 13, 17).

During development, the brain vascular network is established during embryogenesis and at the postnatal stage (11, 26). After initial formation of the perineural vascular plexus (PNVP)

surrounding the CNS via vasculogenesis (= *de novo* formation of blood vessels from angioblasts), the brain is predominantly vascularized by sprouting angiogenesis (= formation of new blood vessels from pre-existing ones) (11, 26). During sprouting angiogenesis, endothelial tip cells (ETCs) at the forefront of vascular sprouts extend filopodia to guide the growing vessels (11, 27, 28). (see Supplementary Introduction). However, even though peri-/neurovascular crosstalk and metabolism are crucial features of brain tumors (4, 5, 7, 8, 29-35), less is known about how developmental signaling pathways are reactivated in brain tumors to regulate angiogenesis, and endothelial metabolism (4, 8, 31, 32).

The reactivation of fetal signaling programs in tumor tissues is defined as the onco-fetal axis and has been described in cancer cells in brain and peripheral tumors (18-24) as well as in endothelial cells in liver cancer (25). However, the relevance of the onco-fetal axis in endothelial- and perivascular cells of the brain vasculature in human (glial) brain tumors is currently unknown. Onco-fetal programs represent interesting therapeutic targets as they are upregulated in the brain tumor tissue as compared to the surrounding healthy brain, thereby reducing the likelihood of side-effects (36). Thus, a better understanding of the onco-fetal axis in the (glial) brain tumor vasculature harbors great scientific and translational potential, including the identification of novel therapeutic targets.

Nucleolin (NCL) is a multifunctional and widely expressed protein found in various cell compartments of eukaryotic cells (nucleoplasm, nucleolus, cytoplasm and plasma membrane) (37) and its main functions are the regulation of ribosome biogenesis and ribosomal RNA (rRNA) synthesis (38-40), while it also regulates cell cycle, senescence, apoptosis, and angiogenesis (37, 38, 41). Nucleolin expression increases with malignancy grade and proliferation rate in both human and mouse glial brain tumors (42-45), indicating its pro-proliferative role in glioma (see Supplementary Introduction). Targeting Nucleolin in cancer cells using the anti-Nucleolin aptamer AS1411 has been reported in brain and peripheral tumors (46-48), whereas AS1411-mediated

targeting of Nucleolin in ECs of the pathological vasculature in the retina resulted in reduced angiogenicity (49, 50). However, AS1411 has not been used to target Nucleolin in the vasculature of tumors in- and outside the CNS. In peripheral tissues, Nucleolin was shown to be upregulated at the cell surface of ECs in angiogenic vessels in breast tumors (51), with regulatory effects on carcinogenesis and angiogenesis, and to regulate EC motility and tube formation *in vitro* (52). Moreover, targeting endothelial Nucleolin induced endothelial apoptosis and vessel normalization in a pancreatic tumor mouse model (53, 54). However, the role of Nucleolin on angiogenesis and EC function in the developing human brain and in human gliomas remains poorly understood. Here, using a variety of in vivo and *in vitro* assays, we show that Nucleolin is an onco-fetal protein in human gliomas regulating sprouting angiogenesis and endothelial metabolism.

RESULTS

Nucleolin is a neurodevelopmental protein of the onco-fetal axis that is silenced in the healthy adult brain and reactivated in the NVU/PVN of glial brain tumors

To investigate whether Nucleolin constitutes a neurodevelopmental protein that is reactivated in brain tumors, we performed immunofluorescence microscopy of the main NVU/PVN cellular components of human fetal brain, of human normal adult brain, and of human glial brain tumors. Nucleolin was highly expressed during fetal forebrain neocortex development, at gestational week 18 (GW18) and GW22, significantly downregulated in the adult brain, and upregulated in brain tumors, as revealed by immunofluorescence staining against Nucleolin and the nuclear marker TO-PRO-3 (55) (Figure 1A-C,P). Moreover, Nucleolin expression was present throughout the nucleoplasm during fetal development but was restricted to the nucleolus in the adult human brain (Figure 1A,B). In GBM, Nucleolin expression was detected across the entire nucleoplasm and appeared similar to the pattern observed during fetal development (Figure 1A,C). Within the NVU, Nucleolin was expressed in both endothelial- and perivascular cells (Figure 1D-O). Nucleolin was highly expressed in cells labeled with the endothelial marker cluster of differentiation 31 (CD31) during brain development, where 84% of $CD31^+$ ECs showed Nucleolin expression across the entire nucleoplasm (Figure 1D, Q). Nucleolin was significantly downregulated in the adult brain with 16% of the $CD31^+$cells being $Nucleolin^+$ ECs (predominant nucleolar expression) (Figure 1E,Q), but was significantly upregulated in GBM ECs, where 67% of the $CD31^+$ were $Nucleolin^+$ (nucleoplasm and nucleolar expression), similar to its expression in fetal brain (Figure 1D,F,Q). Nucleolin was also highly expressed in $CD105^+$ angiogenic ECs during fetal brain development and in GBM, with 75% and 74% $CD105^+$/$Nucleolin^+$ double-positive ECs, respectively (Figure 1G,I,R), whereas only 13% $CD105^+$/$Nucleolin^+$ ECs could be observed in adult brain slices (Figure 1H,R), consistent with the reported quiescence of ECs in the adult normal brain (11, 56, 57).

Within the NVU, blood vessel endothelial cells are in contact with perivascular supportive cells such as pericytes, astrocytes, and neuronal stem cells (11, 57-61). Therefore, we assessed the expression of Nucleolin in pericytes and perivascular astrocytes. Glial fibrillary acidic protein $(GFAP)^+$ astrocytes formed typical patterns by contacting ECs and showed very strong Nucleolin expression during fetal brain development with 95% of $GFAP^+$/$Nucleolin^+$ astrocytes (Figure 1J,S). In contrast, in the adult brain, Nucleolin was significantly downregulated in $GFAP^+$ astrocytes with only 24% $GFAP^+$/$Nucleolin^+$ (no restriction to nucleolus observed), but showed a significant upregulation in glioblastoma with 84% of $GFAP^+$/$Nucleolin^+$ astrocytes (Figure 1J,K,S). Interestingly, neuron-glial antigen 2 positive ($NG2^+$) pericytes showed low Nucleolin expression in fetal brain development with only 13% $NG2^+$/$Nucleolin^+$ pericytes as well as in the adult brain with 7% $NG2^+$/$Nucleolin^+$ pericytes (Figure 1M,N,T). However, Nucleolin was significantly upregulated in human glioblastoma with 57% $NG2^+$/$Nucleolin^+$ pericytes (Figure 1O,T).

Taken together, these data reveal that Nucleolin is highly expressed in endothelial- and certain NVU cells (astrocytes > pericytes) during fetal brain development, is subsequently downregulated in the adult brain, and is reactivated in GBM. This characterizes Nucleolin as an onco-fetal protein that is reactivated in human glial brain tumors after downregulation in the quiescent adult NVU (18-25).

Nucleolin expression within the NVU correlates with glial brain tumor malignancy and progression

In order to address the expression of Nucleolin in glial brain tumor progression (from WHO low- to high-grade tumors (62-64), we referred to tissue microarrays (TMAs) of human glioma stained immunohistochemically for Nucleolin and the nuclear marker Mayer's hemalum (Figure 2A-D). Nucleolin expression was markedly upregulated in human glial brain tumors as compared to the adult normal brain (Figure 2A-E). Moreover, Nucleolin expression was significantly increased

during glial tumor progression, ranging from 32% of Nucleolin$^+$ cells in WHO grade I glioma to 57% in glioma grade IV (= glioblastoma) (Figure 2E). Nucleolin showed a significant upregulation from low- grade (WHO grade I and II) to high-grade glioma (WHO grade III) as well as a significant increase from WHO grade III to WHO grade IV glioma (Figure 2A-D, F). In recurrent glioblastoma, Nucleolin expression showed a slight but significant decrease as compared to primary glioblastoma (Figure 2E). Nucleolin expression correlated well with the established proliferation marker Ki-67 (65) in all glioma grades (Figure 2G).

Based on Nucleolin expression within perivascular cells of the developmental- and tumoral NVU, we next addressed its effects on tumoral cell proliferation. To determine whether Nucleolin promotes GBM cell proliferation, Nucleolin was knocked down in the human glioblastoma cell lines LN-229 (66) and LN-18 (67) as well as in freshly isolated primary human glioblastoma cells (GBM-1) using siRNA (Figure 2I-K). Cell proliferation of LN-229, LN-18, and GBM-1 was inhibited by siRNA-mediated knock-down of Nucleolin (Figure 2H) compared with scrambled controls, in agreement with the previously reported strong pro-proliferative effect of Nucleolin in human glioblastoma cells (42, 68).

Next, we examined the expression of Nucleolin in tumor blood vessels referring to spatial transcriptomics and immunohistochemistry. In agreement with our immunofluorescent data in GBMs (see Figure 1F,Q), exploratory spatial transcriptomics in human GBMs showed co-occurrence of Nucleolin and various endothelial markers including CD31 (*PECAM1*), CD105 (*ENG*), *CLDN5* and *VWF* (Supplementary Figure 1A-L). Moreover, Nucleolin was indeed present in the wall of tumor blood vessels, showing an increased expression during glial tumor progression (WHO I – IV, Figure 2L-O), further suggesting a regulatory effect on human glial brain tumor angiogenesis.

Taken together, these data indicate that Nucleolin expression is reactivated in tumor cells and tumor endothelial cells within the NVU during human astrocytic tumor progression.

Nucleolin is expressed within the NVU and in sprouting ETCs, and promotes the number of tip cell filopodia during brain development in vivo

Nucleolin has been shown to affect tumor and blood vessel growth in peripheral tissues (42, 51, 52, 68, 69), but whether it regulates sprouting angiogenesis during brain development remains unknown. To assess whether Nucleolin affects sprouting angiogenesis and ETCs during brain development, we addressed Nucleolin expression in the vicinity of sprouting blood vessels in the human fetal brain. CD105-labeled ETCs with their typical, finger-like protruding filopodia could be recognized in GW 18 and 22 human fetal brain forebrains (Figure 3A-D). Nucleolin was expressed in $CD105^+$ endothelial tip-, stalk-, and phalanx cells (Figure 3A-D) as well as in perivascular cells surrounding sprouting capillary ETCs (filopodia) (Figure 3A-D). We observed Nucleolin in nuclei of $CD105^+$ endothelial tip-, stalk-, and phalanx cells but not on the (endothelial- and perivascular) cell surface and not in filopodia protrusions (Figure 3A-D).

We examined whether Nucleolin expression affected the number of ETC filopodia and observed a lower number of filopodia in ETCs with low Nucleolin expression (Figure 3E,F) and a higher number of filopodia in ETCs with high Nucleolin expression (Figure 3G,H). Accordingly, we quantified the number of filopodia per $Nucleolin^+/CD105^+$ ETCs and assessed Nucleolin expression for each ETC. Indeed, the number of filopodia positively correlated with Nucleolin expression in the ETCs, as revealed by median fluorescent intensity (Figure 3I). These results strongly suggest that Nucleolin positively regulates the number of ETC filopodia in the human fetal brain.

Nucleolin promotes HCMEC and HUVEC sprouting angiogenesis in vitro

Based on these expression studies suggesting a role for Nucleolin in sprouting angiogenesis and ETC filopodia in vivo, we next investigated the functional role of Nucleolin in human angiogenic

endothelial cell sprouting in vitro. We used siRNA to knock-down Nucleolin in human cerebral microvascular endothelial cells HCMEC/D3 (HCMECs) and human umbilical vein endothelial cells (HUVECs) (Figure 4A-G, Supplementary Figure 2A-G). In Nucleolin siRNA-treated HCMECs ($HCMEC^{Nucleolin\ KD}$) and HUVECs ($HUVEC^{Nucleolin\ KD}$), Nucleolin expression was decreased and confined to the nucleolus when compared to the siRNA control-treated HCMECs ($HCMEC^{Control\ KD}$) and HUVECs ($HUVEC^{Control\ KD}$, Figure 4A-D, Supplementary Figure 2A-D). Accordingly, qRT-PCR and Western blot analysis revealed significant knocking down of Nucleolin at both the mRNA- and the protein levels in HCMECs and HUVECs (Figure 4E-G, Supplementary Figure 2E-G).

To test the effects of Nucleolin on sprouting angiogenesis in vitro, we referred to an in vitro spheroid angiogenesis assay (70). HCMECs and HUVECs in the sprouting spheroid assay grew vessel-like sprouts composed of multiple branches in the control group (Figure 4H,I, Supplementary Figure 2H,I). In contrast, siRNA-mediated knock-down of Nucleolin markedly suppressed the number of vessel sprouts per spheroid as well as the length of the sprouts as compared to the control group in both cell types (Figure 4J-M, Supplementary Figure 2J-M), suggesting a promoting effect on sprouting angiogenesis.

Given the important role of Nucleolin in cell proliferation (37, 39, 40), we next assessed whether Nucleolin affects EC proliferation in a 3HT proliferation assay. Indeed, HCMEC and HUVEC proliferation was significantly reduced upon siRNA-mediated Nucleolin knock-down (Figure 4N, Supplementary Figure 2N), indicating a positive regulatory role for Nucleolin on HCMEC and HUVEC cell proliferation, reminiscent of stalk cell behavior in vivo (11, 27, 57).

Because we observed Nucleolin expression in brain ECs (Figure 1D-F, and Figure 4A-D), based on its positive effects on (brain) EC proliferation (Figure 4N, Supplementary Figure 2N), and given that Nucleolin has been targeted in cancer cells and retinal endothelial cells using the aptamer AS1411(45-50, 71, 72), we next tested the effects of the Nucleolin-specific aptamer AS1411 on

brain EC proliferation. Treatment of HCMECs using 1.25, 5 and 10μM of AS1411 dose-dependently inhibited their proliferation after 96h (Figure 4O). Taken together, these results suggest that endothelial Nucleolin is a positive regulator of sprouting angiogenesis, endothelial proliferation-, and filopodia formation in the brain that can potentially be targeted in brain ECs using aptamers.

Nucleolin regulates HCMEC and HUVEC lamellipodia and filopodia formation and actin cytoskeleton orientation

Lamellipodia and filopodia are composed of actin and myosin fibers, and are essential components of in vivo sprouting angiogenesis (28). Therefore, to further assess the effects of Nucleolin on HCMEC and HUVEC angiogenesis in vitro, we addressed cell shape and morphology as well as actin orientation after Nucleolin knock-down (Figure 5A-K, Supplementary Figure 3A-K). HCMEC$^{\text{Nucleolin KD}}$ and HUVEC$^{\text{Nucleolin KD}}$ spread less and were not as elongated as control cells as quantified by their increased cell circularity and decreased cell area (Figure 5I,J, Supplementary Figure 3I,J). F-Actin fibers were more randomly organized in the HCMEC$^{\text{Nucleolin KD}}$ and HUVEC$^{\text{Nucleolin KD}}$ (Figure 5C,F, Supplementary Figure 3C,F). Accordingly, the distribution of actin orientation showed a classical peak in controls, whereas in the HCMEC$^{\text{Nucleolin KD}}$ and HUVEC$^{\text{Nucleolin KD}}$ the actin orientation was more randomly distributed (Figure 5K, Supplementary Figure 3K), indicating the HCMEC$^{\text{Nucleolin KD}}$ and HUVEC$^{\text{Nucleolin KD}}$ had poorly orientated stress fibers as opposed to well-aligned stress fibers of control cells.

To assess the effects of Nucleolin on HCMECs and HUVECs and their filopodia, we cultured these cells on a substrate consisting of nanopillar arrays (73, 74) (Figure 6A-C, Supplementary Figure 4A-C) allowing assessment of filopodia dynamics and traction/pulling forces exerted by the spreading of HCMECs and HUVECs on the substrate (Figure 6D-G, Supplementary Figure 4D-G). In HCMEC$^{\text{Nucleolin KD}}$ and HUVEC$^{\text{Nucleolin KD}}$, the number of filopodial extensions per cell was

significantly reduced as compared to HCMEC$^{Control\ KD}$ and HUVEC$^{Control\ KD}$ (Figure 6D,F,H, Supplementary Figure 4D,F,H).

Next, we examined the movement of Nucleolin-siRNA treated HCMECs and HUVECs on the nanopillar surface. In HCMEC$^{Nucleolin\ KD}$ and HUVEC$^{Nucleolin\ KD}$, the mean displacements of the nanopillars were significantly decreased as compared to the control group (0.061 µm and 0.129 µm and 0.068 µm and 0.136 µm, respectively, Figure 6E,G,I, Supplementary Figure 4E,G,I). HCMEC$^{Nucleolin\ KD}$ and HUVEC$^{Nucleolin\ KD}$ exerted significantly reduced average traction forces of 4.8nN and 5.4 nN when compared to the control HCMECs and HUVECs (10.1 nN and 10.7 nN, respectively, Figure 6J, Supplementary Figure 4J). These results indicate a pro-adhesive / pro-migratory / pro-explorative effect of Nucleolin on endothelial cells and their filopodial protrusions. These data indicate that Nucleolin is important for actin orientation and polarization which is required for EC lamellipodia- and filopodia formation, structures that are crucial for migration, proliferation, and sprouting of vascular ECs in vivo.

Bulk RNA sequencing (RNAseq) reveals regulation of angiogenic pathways including VEGF-A-VEGFR2 as well as of endothelial metabolism upon Nucleolin knock-down

To address the downstream signaling pathways induced by Nucleolin in human ECs, we performed an unbiased transcriptome analysis by RNA sequencing of HCMEC$^{Nucleolin\ KD}$ and HCMEC$^{Control\ KD}$ as well as of HUVEC$^{Nucleolin\ KD}$ and HUVEC$^{Control\ KD}$. RNAseq revealed 445 and 3240 significantly differentially regulated genes between HCMEC$^{Nucleolin\ KD}$ and HCMEC$^{Control\ KD}$ and between HUVECs$^{Nucleolin\ KD}$ and HUVECs$^{Control\ KD}$, respectively (Figure 7A-C, Supplementary Figure 5A-C). Analysis of the gene expression by the fragments per kilobase of exon model per million reads mapped (FPKM) values confirmed Nucleolin downregulation mediated by siRNA in HCMECs and HUVECs (Figure 7D, Supplementary Figure 5D). In HCMECs$^{Nucleolin\ KD}$, genes involved in

inflammatory responses including *IL17D* and *CCL2* (75) were among the top-regulated genes (Figure 7E; regarding HUVECs, see Supplementary Results).

Next, to address the molecular pathways regulated by Nucleolin in ECs, we performed gene set enrichment analyses (GSEA) (76) between siNCL-treated HCMECs/HUVECs and the control HCMECs/HUVECs, respectively. In HCMEC$^{\text{Nucleolin KD}}$, GSEA followed by pathway visualization using cytoscape (77) revealed that upregulated genes were mainly involved in regulation of angiogenesis and immune-related processes, while the downregulated genes were linked to regulation of metabolic processes, and translation (Figure 7F). Indeed, angiogenesis and vascular development were significantly enriched upon Nucleolin depletion in HCMECs whereas oxidative phosphorylation and glycolysis showed significant enrichment in control HCMECs (Figure 7F-J). We next examined genes driving the enrichment of regulation of angiogenesis and glycolysis and oxidative phosphorylation in brain ECs. Genes involved in the key angiogenic *VEGFA-VEGFR2* pathway including *VEGFR2* as well as the *VEGFA-VEGFR2* regulatory genes *KLF4* (78), *ANGPTL4* (79), *TEK (80)* and *SPHK1* (81) were significantly upregulated, whereas genes involved in the regulation of glucose metabolism such as *HK2* (82), *ALDOC* (83), *ENO2* (84), *PFKL* (85), *PFKP* (86) were significantly downregulated in HCMEC$^{\text{Nucleolin KD}}$ (Figure 8A,B), indicating that Nucleolin regulates those genes involved in angiogenic sprouting in brain ECs. Importantly, we observed overlapping genes regulating angiogenesis (*VEGFR2*, *KLF4*, *ANGPTL4*, *TIE2* and *SPHK1*) and metabolic processes (*HK2*, *ENO2*, *PFKL*) in the two cell types following Nucleolin depletion (Supplementary Figure 6A,B), suggesting common underlying mechanisms driving vascular growth and endothelial metabolism in HCMECs and HUVECs (regarding HUVECs, see Supplementary Results).

Based on the observed regulatory effect of Nucleolin on sprouting angiogenesis, we next analyzed the expression of main regulators of the key angiogenic pathways VEGF-A/VEGFR2/3-Dll4-Jagged-Notch and Hippo-YAP-TAZ-. We observed regulation of the central VEGF-A-VEGFR2

pathway, upregulation of the anti-angiogenic Dll4-Notch as well downregulation of the pro-angiogenic Hippo-YAP-TAZ pathway upon Nucleolin-KD (Figure 8C-E, Supplementary Figure 6C-E, Supplementary Results), supporting the pro-angiogenic role of Nucleolin in brain and peripheral ECs.

Finally, given its central role in angiogenesis and vascular growth and based on its regulation in the bulkRNAseq data, we validated the alteration of transcriptional expression of *VEGFR2* at the protein level using immunofluorescence in both cell types. We observed decreased expression of the phosphorylated form of VEGFR2 (p-VEGFR2) in $HCMEC^{Nucleolin\ KD}$ and $HUVEC^{Nucleolin\ KD}$ (Figure 8F-O, Supplementary Figure 6F-O), thereby indicating a positive regulatory effect of Nucleolin on VEGFR2 and suggesting a potential crosstalk between the VEGF-A-VEGFR2 and Nucleolin pathways in brain and peripheral ECs. Taken together, these results suggest that Nucleolin's positive regulatory effects on CNS sprouting angiogenesis and endothelial metabolism might be regulated by interaction with the *VEGFA-VEGFR2* pathway and with glycolytic enzymes including *HK2*.

Metabolomics confirm regulation of endothelial glucose metabolism upon Nucleolin knock-down

Endothelial metabolism is a crucial regulator of sprouting angiogenesis, ETC formation, and endothelial lamellipodia- and filopodia-dynamics (87-90). Moreover, endothelial cell glycolysis regulates the rearrangement of ECs by promoting filopodia formation and by reducing intercellular adhesion (90). Based on the regulation of metabolic pathways upon Nucleolin knock-down in our bulkRNAseq data as well as on the observed regulatory effects of Nucleolin on sprouting angiogenesis, ETC (filopodia) and the actin cytoskeleton, we next investigated whether Nucleolin affected endothelial glucose and fatty acid metabolism (89). Therefore, we performed unbiased metabolic profiling using liquid chromatography tandem mass spectrometry (LC-MS/MS) (91) in

HCMEC$^{Nucleolin\ KD}$ / HUVEC$^{Nucleolin\ KD}$ compared to HCMEC$^{Control\ KD}$ / HUVEC$^{Control\ KD}$ (Figure 9A-F, Supplementary Figure 9A-F). Hierarchical clustering revealed that metabolite levels of HCMEC$^{Nucleolin\ KD}$ and HUVEC$^{Nucleolin\ KD}$ clearly separated from HCMEC$^{Control\ KD}$ and HUVEC$^{Control\ KD}$, revealing significantly regulated metabolites between the groups (Figure 9A,B, Supplementary Figure 9A,B). This analysis showed 747 and 383 metabolites altered by the knock-down of Nucleolin in HCMEC and HUVECs, respectively (Figure 9B, Supplementary Figure 9B). Principal component analysis (PCA) further identified specific groups of metabolites including those involved in endothelial glucose metabolism to be different in HCMEC$^{Nucleolin\ KD}$ and HUVEC$^{Nucleolin\ KD}$ as compared to the control groups (Figure 9C,D, Supplementary Figure 9C,D). Next, we examined the metabolic pathways regulated by Nucleolin in ECs. GSEA (76) revealed glycolysis and fatty acid metabolism pathways to be downregulated in HUVEC$^{Nucleolin\ KD}$ and fatty acid metabolism pathways to be downregulated in HCMEC$^{Nucleolin\ KD}$ (Figure 9E, Supplementary Figure 9E). Moreover, glycolysis was downregulated (even though not significantly) in HCMEC$^{Nucleolin\ KD}$ (Figure 9E). We next analyzed the abundance of metabolites involved in glycolysis and other metabolic pathways important for EC homeostasis and activation (89) (Figure 9F, Supplementary Figure 9F, Supplementary Figure 10) . Interestingly, we found that among the eight glucose metabolites detected in HCMECs and HUVECs, Glyceraldehyde 3-phosphate (G3P), Phosphoenolpyruvate (PEP) and Lactate (Lac) were significantly decreased in HCMEC$^{Nucleolin\ KD}$, whereas lactate was significantly decreased in HUVEC$^{Nucleolin\ KD}$ (Figure 9F, Supplementary Figure 9F). Notably, lactate levels were decreased by 35% in HCMEC$^{Nucleolin\ KD}$ versus HCMEC$^{Control\ KD}$ and by 55% in HUVEC$^{Nucleolin\ KD}$ versus HUVEC$^{Control\ KD}$, respectively (Figure 9F, Supplementary Figure 9F). Moreover, the NADH/NAD$^+$ ratio indicating for metabolic activity (92, 93) showed a decrease (although not significant) upon Nucleolin KD in both cell types (Figure 9F, Supplementary Figure 7f). Together, these results indicate that Nucleolin exerts its positive

regulatory effects on CNS sprouting angiogenesis via positive regulation of endothelial (glucose) metabolism.

Nucleolin regulates endothelial glucose-, but not fatty acid metabolism

To further examine the observed effects of Nucleolin on endothelial metabolism, we next performed functional metabolic assays addressing endothelial glucose and fatty acid metabolism in HCMECs and HUVECs. Using a glycolytic flux assay (94), siRNA-mediated knock-down of Nucleolin resulted in a significant reduction of glycolysis as compared to the control HCMECs and HUVECs (Figure 10A, Supplementary Figure 11A). Similarly, $HCMEC^{Nucleolin\ KD}$ and $HUVEC^{Nucleolin\ KD}$ showed reduced glucose uptake and decreased lactate production as compared to the $HCMEC^{Nucleolin\ KD}$ and $HUVEC^{Control\ KD}$ (Figure 10B,C, Supplementary Figure 11B,C), indicating a positive regulatory effect of Nucleolin on HCMEC and HUVEC glucose metabolism. 6-phosphofructo-2-kinase/fructose-2,6-biphosphatase 3 (PFKFB3), and HK2, have been shown to be key regulators of endothelial glucose metabolism (88, 89). To address whether Nucleolin affected the expression patterns of these genes in HCMECs and HUVECs, we performed qRT-PCR and Western blots of $HCMEC^{Nucleolin\ KD}$ and $HUVEC^{Nucleolin\ KD}$ and $HCMEC^{Control\ KD}$ and $HUVEC^{Control\ KD}$. HK2 was significantly downregulated upon Nucleolin knock-down on the mRNA level (Figure 10D, Supplementary Figure 11D), whereas PFKFB3 showed no significant change on both the mRNA and the protein levels (Figure 10E-J, Supplementary Figure 11E-J).

Next, we assessed whether Nucleolin also regulates endothelial fatty acid oxidation (FAO) which is known to exert crucial effects on endothelial stalk cells proliferation (89, 95), and to be upregulated in quiescent ECs as a protection against oxidative stress (96). Nucleolin KD in HCMECs and HUVECs did not affect endothelial fatty acid oxidation (Figure 10K, Supplementary Figure 11K). Carnitine palmitoyltransferase 1A (CPT1a) has been shown to be a key regulator of endothelial fatty acid metabolism (88, 89). As expected, qRT-PCR and Western blot analysis of

HCMEC$^{\text{Nucleolin KD}}$ and HUVEC$^{\text{Nucleolin KD}}$ showed no significant differences of CPT1a as compared to the HCMEC$^{\text{Control KD}}$ and HUVEC$^{\text{Control KD}}$ groups at both the mRNA- and protein- levels (Figure 10L-N, Supplementary Figure 11L-N).

Taken together, these data reveal that KD of Nucleolin decreases endothelial glucose metabolism without affecting endothelial fatty acid metabolism, indicating a positive regulatory role of Nucleolin on sprouting angiogenesis via promoting endothelial glucose metabolism.

DISCUSSION

Here, using in vitro and in vivo approaches, we show that Nucleolin is a positive regulator of angiogenesis in the human fetal brain. Our results suggest that Nucleolin promotes brain endothelial sprouting, -proliferation, and -filopodia formation potentially via interaction with the VEGF-VEGFR2 pathway and positively regulates brain endothelial glucose metabolism via the regulation of glycolytic enzymes including HK2. We propose that, by acting on the cytoskeleton of CNS endothelial (tip- and stalk) cells and their filopodia, and by regulating vascular endothelial metabolism, Nucleolin controls the sprouting and filopodia extension of growing CNS blood vessels during human fetal brain development, and presumably in human brain tumors. Importantly, the characterization of Nucleolin as an onco-fetal protein in the brain tumor vasculature and its inhibition using aptamers identifies Nucleolin as a potential pharmaceutical target for gliomas.

Nucleolin - a putative NVU/PVN derived onco-fetal signal to regulate developmental brain- and brain tumor (vascular) growth?

Most of the evidence regarding the molecular regulation of sprouting angiogenesis during brain development is based on murine studies (97, 98), whereas less knowledge exists how the vascularization and ETCs are regulated in the human brain. Interestingly, angiogenesis is highly dynamic during brain development and almost quiescent in the adult healthy brain (11, 14, 57), but is reactivated in a variety of angiogenesis-dependent CNS pathologies such as brain tumors, brain vascular malformations, or stroke (4, 5, 14), thereby activating endothelial- and perivascular cells of the NVU (7, 11, 57). In our study, we not only observed a reactivation of Nucleolin in angiogenic endothelial- and perivascular cells within glial brain tumors but also a positive correlation of Nucleolin expression with astrocytic tumor progression, in agreement with (99), suggesting a crucial role of Nucleolin as a perivascular niche-derived signal in both angiogenic- and tumor

growth. The perivascular niche has been shown to activate tumor growth in mouse- and zebrafish models of breast cancer (100). Strikingly, endothelial-derived thrombospondin-1 in the stable microvasculature induced sustained breast cancer cell quiescence but this suppressive cue was lost in sprouting neovasculature, where ETC-derived active TGF-β1 and periostin promoted breast tumor growth (100). These characterized the stable microvasculature as a "dormant perivascular (tumor) niche" in contrast to the sprouting neovasculature which constitutes an "activated perivascular (tumor) niche" in which ETCs exert crucial roles. In light of these studies, the exploration of Nucleolin's angiogenic function within the perivascular tip cell niche in vivo promises to be an exciting avenue for future investigations.

Here, we found that Nucleolin is an important positive regulator of angiogenesis and ETC filopodia in human fetal brain. The expression of Nucleolin in endothelial- and perivascular cells such as astrocytes and pericytes within the neurovascular unit of the human fetal brain, its downregulation in the adult healthy brain and reactivation in brain tumors characterizes Nucleolin as an onco-fetal protein and suggests an integral role once reactivated during brain cancer. Its high expression in $CD105^{+}$ angiogenic blood vessel ECs in both human fetal brain and human glioblastoma (but not in the adult healthy brain) supports this presumed role in active (developmental, tumor) versus stable (adult healthy) brain angiogenesis. Accordingly, our in vitro results suggest that by exerting stimulatory effects on sprouting angiogenesis, filopodia extension, and glucose metabolism of vascular ECs, Nucleolin might promote the sprouting of angiogenic blood vessel ECs into the brain parenchyma. The latter is also strongly suggested by the positive correlation between Nucleolin expression and the number of ETC filopodia in the fetal brain parenchyma in vivo. Other neurodevelopmental regulators such as VEGF-A, and GPR124 are downregulated in the adult healthy CNS and are reactivated in vascular-dependent CNS pathologies such as brain tumors or stroke (101-103). However, in contrast to those angiogenic factors, Nucleolin is one of the first to have been directly compared in both human fetal brain and human gliomas. Furthermore, Nucleolin

endothelial- and perivascular expression within the fetal- and tumor perivascular niche and its presumed different roles on the involved cell types (angiogenesis vs. tumor growth) characterize Nucleolin as an important developmental signal reactivated during brain tumor growth and in consequence as an onco-fetal protein.

Nucleolin as regulator of glucose-, but not fatty acid endothelial metabolism – effects on endothelial tip- and stalk cells?

Endothelial metabolism has recently emerged as a crucial regulator of sprouting angiogenesis during development and in tumors (87-89, 95, 104, 105). Moreover, it was suggested that endothelial tip cells mainly rely on glycolysis whereas endothelial stalk cells also use fatty acid metabolism to support proliferation (87-89, 95, 104, 105). Here, we found that Nucleolin positively regulates endothelial glycolysis- but not fatty acid metabolism in vitro, indicating that Nucleolin's main effect might be on tip cells, but Nucleolin's precise roles on both tip- and stalk cells in- and outside the CNS, for instance in the embryonic or postnatal brain (26, 57) or in the postnatal retina (106) need to be investigated in vivo (see Supplementary Discussion).

As also demonstrated by our bulk RNA sequencing, pathways regulated downstream of Nucleolin were linked to angiogenesis and endothelial glucose metabolism. While the observed regulatory effects of Nucleolin on endothelial glucose metabolism are in line with an important role of glycolysis in angiogenesis and vascular biology in- and outside the CNS (88, 89, 104, 107, 108), we cannot exclude that Nucleolin regulates other metabolic pathways that participate in (brain) angiogenesis and (brain) EC biology. Thus, given the crucial role of endothelial metabolism for vessel sprouting in development and disease (87, 88, 104) as well as of tumor metabolism in gliomas (35), investigating the precise role of Nucleolin on EC metabolism and angiogenesis in the human brain vasculature along the onco-fetal axis promises to be exciting.

A putative role for Nucleolin in angiogenesis-dependent CNS pathologies via molecular crosstalk with the VEGF-VEGFR signaling axis?

Angiogenesis and the perivascular niche exert crucial roles in the pathophysiology of various vascular-dependent CNS diseases such as brain tumors, vascular malformations, and stroke (6, 7, 17, 49, 50, 56). With regard to brain tumors, glycosylated surface Nucleolin has been shown to increase with the malignancy grade of human gliomas (99). A high expression of Nucleolin may therefore promote vascularization of astrocytoma and thereby promote brain tumor growth (see Supplementary Discussion). Furthermore, the anticancer aptamer AS1411 - that binds specifically to Nucleolin - has shown promising clinical activity and is being widely used as a tumor-targeting agent (72) as well as an inhibitor of pathological angiogenesis in the retina (49, 50). In line with these reports, we find AS1411-mediated inhibition of brain EC proliferation in vitro, indicating that AS1411 could be tested to target the brain tumor vasculature in vivo. Interestingly, antibody- and peptide-mediated targeting of Nucleolin induced normalization of tumor vasculature in pancreas- and breast cancer models (53, 69), further suggesting that strategies targeting Nucleolin might affect the glioblastoma vasculature. During (glial) brain tumor progression, vascular dysfunction is partially mediated via angiogenic factors including VEGF-VEGFR (17, 109-111) and blocking VEGF-VEGFR signaling results in transient normalization of the immature and leaky brain tumor vasculature and to survival benefits in patients with newly diagnosed as well as recurrent glioblastoma (17, 112, 113). Here, we observed a positive regulatory effect of Nucleolin on the VEGF-VEGFR2 pathway in vitro, indicative of a molecular crosstalk between these two signaling axes. Given that both pathways regulate angiogenesis and vascular normalization, combinatorial targeting of Nucleolin and VEGF-VEGFR2 to normalize the brain tumor vasculature may be a promising antiangiogenic strategy for glioblastoma patients. Taken together, these literature indications in concert with our data suggest that - in addition to its effect on tumor cell

proliferation - onco-fetal Nucleolin may regulate brain tumor vascularization and could be a candidate for targeted therapy on both tumor and endothelial cells in human gliomas.

MATERIALS AND METHODS

Additional detailed methods can be found in Supplementary Methods.

Study approval

Tissue samples from human fetal brains were obtained from post-mortem fetuses derived from spontaneous abortions and received by the Department of Pathological Anatomy, University of Bari School of Medicine. Tissue preparation and storage were performed as previously described. The study was approved by the Ethics Committee of the University of Bari Medical School and complied with the principles stated in the Declaration of Helsinki.

Tissue samples from human glioblastoma patients and controls from temporal lobes after selective temporal-lobectomy in patients with chronic pharmaco-resistant mesial temporal lobe epilepsy, were obtained during surgery at the Department of Neurosurgery, University Hospital Zurich. Written informed consent was obtained from patients before study entry. All procedures were conducted in accordance with the Declaration of Helsinki and the study was approved by the Ethics Committee of the Canton Zurich.

AUTHOR CONTRIBUTIONS

T.W. had the idea for the study, designed the experiments, wrote the manuscript, and made the figures. T.W., M.S., I.D.T., J-.Y.S., M.G., O.S., F.G., M.E., and M.Y. conducted the experiments and analysed the data. R.S., V.V., D.V., K.D.B., and K.F. supervised the experiments in their respective labs, and T.W. supervised all the research. T.W. wrote the manuscript, M.S. helped editing the manuscript and figures. J.H., O.S., A.M., S.L., J.G., P.M., I.R., K.F., R.S., V.V., D.V., and K.D.B., gave critical inputs to the manuscript. All authors read and approved the final manuscript.

ACKNOWLEDGMENTS

We thank our colleagues Giovanna Longo for help with fetal brain sample preparation for immunofluorescence and confocal imaging, Jiazhuo He for help with in vitro spheroid assays, Hang Zhong for help with the p-VEGFR2/VEGFR2 immunofluorescence image processing and analysis, Hubert Rehrauer for help with bulkRNAseq analysis, Sebastian Streb and Endre Laczko for help with metabolomics analysis, and Nancy Chu Ji for help with the illustrations.

The author(s) disclosed receipt of the following financial support for the research, authorship, and/or publication of this article: T.W. was supported by the OPO Foundation, the Swiss Cancer Research foundation (KFS-3880-02-2016-R, KFS-4758-02-2019-R), the Stiftung zur Krebsbekämpfung, the Kurt und Senta Herrmann Foundation, Forschungskredit of the University of Zurich, the Zurich Cancer League, the Theodor und Ida Herzog Egli Foundation, the Novartis Foundation for Medical-Biological Research, and the HOPE Foundation. K.D.B. was supported by grants of the Swiss National Science Foundation (31003A-176056) and a starting grant of the European Research council (716140). V.V. was supported by the Swiss National Science Foundation (SNF 310030B_133122/1), SNF NCCR "Molecular Systems Engineering", the Commission of the European Communities/European Research Council (ERC) Advanced Grant

(231157), FIRST and SCOPEM facility from ETHZ. D.V. was supported by Intramural Funding (2019).

COMPETING FINANCIAL INTERESTS

The authors declare no competing financial interests.

REFERENCES

1. Batchelor TT, Reardon DA, de Groot JF, Wick W, and Weller M. Antiangiogenic therapy for glioblastoma: current status and future prospects. *Clinical cancer research : an official journal of the American Association for Cancer Research.* 2014;20(22):5612-9.
2. Hegi ME, Diserens AC, Gorlia T, Hamou MF, de Tribolet N, Weller M, et al. MGMT gene silencing and benefit from temozolomide in glioblastoma. *N Engl J Med.* 2005;352(10):997-1003.
3. Stupp R, Mason WP, van den Bent MJ, Weller M, Fisher B, Taphoorn MJ, et al. Radiotherapy plus concomitant and adjuvant temozolomide for glioblastoma. *N Engl J Med.* 2005;352(10):987-96.
4. Carmeliet P, and Jain RK. Molecular mechanisms and clinical applications of angiogenesis. *Nature.* 2011;473(7347):298-307.
5. Jain RK, and Carmeliet P. SnapShot: Tumor angiogenesis. *Cell.* 2012;149(6):1408- e1.
6. Jain RK, di Tomaso E, Duda DG, Loeffler JS, Sorensen AG, and Batchelor TT. Angiogenesis in brain tumours. *Nat Rev Neurosci.* 2007;8(8):610-22.
7. Hjelmeland AB, Lathia JD, Sathornsumetee S, and Rich JN. Twisted tango: brain tumor neurovascular interactions. *Nat Neurosci.* 2011;14(11):1375-81.
8. Jayson GC, Kerbel R, Ellis LM, and Harris AL. Antiangiogenic therapy in oncology: current status and future directions. *Lancet.* 2016;388(10043):518-29.
9. Batchelor TT, Sorensen AG, di Tomaso E, Zhang WT, Duda DG, Cohen KS, et al. AZD2171, a pan-VEGF receptor tyrosine kinase inhibitor, normalizes tumor vasculature and alleviates edema in glioblastoma patients. *Cancer cell.* 2007;11(1):83-95.
10. Gilbert MR, Dignam JJ, Armstrong TS, Wefel JS, Blumenthal DT, Vogelbaum MA, et al. A randomized trial of bevacizumab for newly diagnosed glioblastoma. *N Engl J Med.* 2014;370(8):699-708.
11. Walchli T, Wacker A, Frei K, Regli L, Schwab ME, Hoerstrup SP, et al. Wiring the Vascular Network with Neural Cues: A CNS Perspective. *Neuron.* 2015;87(2):271-96.
12. Weis SM, and Cheresh DA. Tumor angiogenesis: molecular pathways and therapeutic targets. *Nat Med.* 2011;17(11):1359-70.
13. Sweeney MD, Sagare AP, and Zlokovic BV. Blood-brain barrier breakdown in Alzheimer disease and other neurodegenerative disorders. *Nat Rev Neurol.* 2018;14(3):133-50.
14. Potente M, Gerhardt H, and Carmeliet P. Basic and therapeutic aspects of angiogenesis. *Cell.* 2011;146(6):873-87.
15. Wälchli T, Bisschop J, Carmeliet P, Zadeh G, Monnier PP, De Bock K, et al. Shaping the brain vasculature in development and disease in the single-cell era. *Nat Rev Neurosci.* 2022.
16. Walchli T, Bisschop J, Miettinen A, Ulmann-Schuler A, Hintermuller C, Meyer EP, et al. Hierarchical imaging and computational analysis of three-dimensional vascular network architecture in the entire postnatal and adult mouse brain. *Nature protocols.* 2021;16(10):4564-610.
17. Arvanitis CD, Ferraro GB, and Jain RK. The blood-brain barrier and blood-tumour barrier in brain tumours and metastases. *Nat Rev Cancer.* 2020;20(1):26-41.
18. Hsu CC, Chiang CW, Cheng HC, Chang WT, Chou CY, Tsai HW, et al. Identifying LRRC16B as an oncofetal gene with transforming enhancing capability using a combined bioinformatics and experimental approach. *Oncogene.* 2011;30(6):654-67.
19. Khazamipour N, Al-Nakouzi N, Oo HZ, Orum-Madsen M, Steino A, Sorensen PH, et al. Oncofetal Chondroitin Sulfate: A Putative Therapeutic Target in Adult and Pediatric Solid Tumors. *Cells.* 2020;9(4).

20. Oo HZ, Lohinai Z, Khazamipour N, Lo J, Kumar G, Pihl J, et al. Oncofetal Chondroitin Sulfate Is a Highly Expressed Therapeutic Target in Non-Small Cell Lung Cancer. *Cancers (Basel).* 2021;13(17).
21. Vladoiu MC, El-Hamamy I, Donovan LK, Farooq H, Holgado BL, Sundaravadanam Y, et al. Childhood cerebellar tumours mirror conserved fetal transcriptional programs. *Nature.* 2019;572(7767):67-73.
22. Couturier CP, Ayyadhury S, Le PU, Nadaf J, Monlong J, Riva G, et al. Single-cell RNA-seq reveals that glioblastoma recapitulates a normal neurodevelopmental hierarchy. *Nat Commun.* 2020;11(1):3406.
23. Richards LM, Whitley OKN, MacLeod G, Cavalli FMG, Coutinho FJ, Jaramillo JE, et al. Gradient of Developmental and Injury Response transcriptional states defines functional vulnerabilities underpinning glioblastoma heterogeneity. *Nat Cancer.* 2021;2(2):157-73.
24. Huijbers EJM, Khan KA, Kerbel RS, and Griffioen AW. Tumors resurrect an embryonic vascular program to escape immunity. *Sci Immunol.* 2022;7(67):eabm6388.
25. Sharma A, Seow JJW, Dutertre CA, Pai R, Bleriot C, Mishra A, et al. Onco-fetal Reprogramming of Endothelial Cells Drives Immunosuppressive Macrophages in Hepatocellular Carcinoma. *Cell.* 2020;183(2):377-94 e21.
26. Fantin A, Vieira JM, Plein A, Maden CH, and Ruhrberg C. The embryonic mouse hindbrain as a qualitative and quantitative model for studying the molecular and cellular mechanisms of angiogenesis. *Nature protocols.* 2013;8(2):418-29.
27. Gerhardt H, Golding M, Fruttiger M, Ruhrberg C, Lundkvist A, Abramsson A, et al. VEGF guides angiogenic sprouting utilizing endothelial tip cell filopodia. *J Cell Biol.* 2003;161(6):1163-77.
28. De Smet F, Segura I, De Bock K, Hohensinner PJ, and Carmeliet P. Mechanisms of vessel branching: filopodia on endothelial tip cells lead the way. *Arterioscler Thromb Vasc Biol.* 2009;29(5):639-49.
29. Gilbert MR, Wang M, Aldape KD, Stupp R, Hegi ME, Jaeckle KA, et al. Dose-dense temozolomide for newly diagnosed glioblastoma: a randomized phase III clinical trial. *J Clin Oncol.* 2013;31(32):4085-91.
30. Jakobsson L, Franco CA, Bentley K, Collins RT, Ponsioen B, Aspalter IM, et al. Endothelial cells dynamically compete for the tip cell position during angiogenic sprouting. *Nat Cell Biol.* 2010;12(10):943-53.
31. Mazzone M, Dettori D, Leite de Oliveira R, Loges S, Schmidt T, Jonckx B, et al. Heterozygous deficiency of PHD2 restores tumor oxygenation and inhibits metastasis via endothelial normalization. *Cell.* 2009;136(5):839-51.
32. Bergers G, and Benjamin LE. Tumorigenesis and the angiogenic switch. *Nat Rev Cancer.* 2003;3(6):401-10.
33. Ribatti D, and Djonov V. Intussusceptive microvascular growth in tumors. *Cancer Lett.* 2012;316(2):126-31.
34. Frentzas S, Simoneau E, Bridgeman VL, Vermeulen PB, Foo S, Kostaras E, et al. Vessel co-option mediates resistance to anti-angiogenic therapy in liver metastases. *Nat Med.* 2016;22(11):1294-302.
35. Bi J, Chowdhry S, Wu S, Zhang W, Masui K, and Mischel PS. Altered cellular metabolism in gliomas - an emerging landscape of actionable co-dependency targets. *Nat Rev Cancer.* 2020;20(1):57-70.
36. Wälchli T, Ghobrial M, Schwab M, Takada S, Zhong H, Suntharalingham S, et al. Molecular atlas of the human brain vasculature at the single-cell level. *bioRxiv.* 2021:2021.10.18.464715.
37. Tajrishi MM, Tuteja R, and Tuteja N. Nucleolin: The most abundant multifunctional phosphoprotein of nucleolus. *Commun Integr Biol.* 2011;4(3):267-75.

38. Ginisty H, Sicard H, Roger B, and Bouvet P. Structure and functions of nucleolin. *J Cell Sci.* 1999;112 (Pt 6):761-72.
39. Tuteja R, and Tuteja N. Nucleolin: a multifunctional major nucleolar phosphoprotein. *Crit Rev Biochem Mol Biol.* 1998;33(6):407-36.
40. Srivastava M, and Pollard HB. Molecular dissection of nucleolin's role in growth and cell proliferation: new insights. *Faseb J.* 1999;13(14):1911-22.
41. Mongelard F, and Bouvet P. Nucleolin: a multiFACeTed protein. *Trends Cell Biol.* 2007;17(2):80-6.
42. Xu Z, Joshi N, Agarwal A, Dahiya S, Bittner P, Smith E, et al. Knocking down nucleolin expression in gliomas inhibits tumor growth and induces cell cycle arrest. *J Neurooncol.* 2012;108(1):59-67.
43. Goldshmit Y, Trangle SS, Kloog Y, and Pinkas-Kramarski R. Interfering with the interaction between ErbB1, nucleolin and Ras as a potential treatment for glioblastoma. *Oncotarget.* 2014;5(18):8602-13.
44. Benedetti E, Antonosante A, d'Angelo M, Cristiano L, Galzio R, Destouches D, et al. Nucleolin antagonist triggers autophagic cell death in human glioblastoma primary cells and decreased in vivo tumor growth in orthotopic brain tumor model. *Oncotarget.* 2015;6(39):42091-104.
45. Luo Z, Yan Z, Jin K, Pang Q, Jiang T, Lu H, et al. Precise glioblastoma targeting by AS1411 aptamer-functionalized poly (l-gamma-glutamylglutamine)-paclitaxel nanoconjugates. *J Colloid Interface Sci.* 2017;490:783-96.
46. Soundararajan S, Chen W, Spicer EK, Courtenay-Luck N, and Fernandes DJ. The nucleolin targeting aptamer AS1411 destabilizes Bcl-2 messenger RNA in human breast cancer cells. *Cancer Res.* 2008;68(7):2358-65.
47. Rosenberg JE, Bambury RM, Van Allen EM, Drabkin HA, Lara PN, Jr., Harzstark AL, et al. A phase II trial of AS1411 (a novel nucleolin-targeted DNA aptamer) in metastatic renal cell carcinoma. *Invest New Drugs.* 2014;32(1):178-87.
48. Figueiredo J, Lopes-Nunes J, Carvalho J, Antunes F, Ribeiro M, Campello MPC, et al. AS1411 derivatives as carriers of G-quadruplex ligands for cervical cancer cells. *Int J Pharm.* 2019;568:118511.
49. Iturriaga-Goyon E, Vivanco-Rojas O, Magana-Guerrero FS, Buentello-Volante B, Castro-Salas I, Aguayo-Flores JE, et al. AS1411 Nucleolin-Specific Binding Aptamers Reduce Pathological Angiogenesis through Inhibition of Nucleolin Phosphorylation. *Int J Mol Sci.* 2021;22(23).
50. Vivanco-Rojas O, Garcia-Bermudez MY, Iturriaga-Goyon E, Rebollo W, Buentello-Volante B, Magana-Guerrero FS, et al. Corneal neovascularization is inhibited with nucleolin-binding aptamer, AS1411. *Exp Eye Res.* 2020;193:107977.
51. Christian S, Pilch J, Akerman ME, Porkka K, Laakkonen P, and Ruoslahti E. Nucleolin expressed at the cell surface is a marker of endothelial cells in angiogenic blood vessels. *J Cell Biol.* 2003;163(4):871-8.
52. Huang Y, Shi H, Zhou H, Song X, Yuan S, and Luo Y. The angiogenic function of nucleolin is mediated by vascular endothelial growth factor and nonmuscle myosin. *Blood.* 2006;107(9):3564-71.
53. Gilles ME, Maione F, Cossutta M, Carpentier G, Caruana L, Di Maria S, et al. Nucleolin Targeting Impairs the Progression of Pancreatic Cancer and Promotes the Normalization of Tumor Vasculature. *Cancer Res.* 2016;76(24):7181-93.
54. Xu C, Wang Y, Tu Q, Zhang Z, Chen M, Mwangi J, et al. Targeting surface nucleolin induces autophagy-dependent cell death in pancreatic cancer via AMPK activation. *Oncogene.* 2019;38(11):1832-44.

55. Suzuki T, Fujikura K, Higashiyama T, and Takata K. DNA staining for fluorescence and laser confocal microscopy. *J Histochem Cytochem.* 1997;45(1):49-53.
56. Storkebaum E, Quaegebeur A, Vikkula M, and Carmeliet P. Cerebrovascular disorders: molecular insights and therapeutic opportunities. *Nat Neurosci.* 2011;14(11):1390-7.
57. Walchli T, Mateos JM, Weinman O, Babic D, Regli L, Hoerstrup SP, et al. Quantitative assessment of angiogenesis, perfused blood vessels and endothelial tip cells in the postnatal mouse brain. *Nature protocols.* 2015;10(1):53-74.
58. Daneman R, Zhou L, Kebede AA, and Barres BA. Pericytes are required for blood-brain barrier integrity during embryogenesis. *Nature.* 2010;468(7323):562-6.
59. Armulik A, Genove G, Mae M, Nisancioglu MH, Wallgard E, Niaudet C, et al. Pericytes regulate the blood-brain barrier. *Nature.* 2010;468(7323):557-61.
60. Roitbak T, Li L, and Cunningham LA. Neural stem/progenitor cells promote endothelial cell morphogenesis and protect endothelial cells against ischemia via HIF-1alpha-regulated VEGF signaling. *J Cereb Blood Flow Metab.* 2008;28(9):1530-42.
61. Chou CH, Sinden JD, Couraud PO, and Modo M. In vitro modeling of the neurovascular environment by coculturing adult human brain endothelial cells with human neural stem cells. *PLoS One.* 2014;9(9):e106346.
62. Louis DN, Ohgaki H, Wiestler OD, Cavenee WK, Burger PC, Jouvet A, et al. The 2007 WHO classification of tumours of the central nervous system. *Acta Neuropathol.* 2007;114(2):97-109.
63. Louis DN, Perry A, Reifenberger G, von Deimling A, Figarella-Branger D, Cavenee WK, et al. The 2016 World Health Organization Classification of Tumors of the Central Nervous System: a summary. *Acta Neuropathol.* 2016;131(6):803-20.
64. Perry A, and Wesseling P. Histologic classification of gliomas. *Handb Clin Neurol.* 2016;134:71-95.
65. Gerdes J, Lemke H, Baisch H, Wacker HH, Schwab U, and Stein H. Cell cycle analysis of a cell proliferation-associated human nuclear antigen defined by the monoclonal antibody Ki-67. *J Immunol.* 1984;133(4):1710-5.
66. Ishii N, Maier D, Merlo A, Tada M, Sawamura Y, Diserens AC, et al. Frequent co-alterations of TP53, p16/CDKN2A, p14ARF, PTEN tumor suppressor genes in human glioma cell lines. *Brain Pathol.* 1999;9(3):469-79.
67. Diserens AC, de Tribolet N, Martin-Achard A, Gaide AC, Schnegg JF, and Carrel S. Characterization of an established human malignant glioma cell line: LN-18. *Acta Neuropathol.* 1981;53(1):21-8.
68. Destouches D, El Khoury D, Hamma-Kourbali Y, Krust B, Albanese P, Katsoris P, et al. Suppression of tumor growth and angiogenesis by a specific antagonist of the cell-surface expressed nucleolin. *PLoS One.* 2008;3(6):e2518.
69. Fogal V, Sugahara KN, Ruoslahti E, and Christian S. Cell surface nucleolin antagonist causes endothelial cell apoptosis and normalization of tumor vasculature. *Angiogenesis.* 2009;12(1):91-100.
70. Korff T, Krauss T, and Augustin HG. Three-dimensional spheroidal culture of cytotrophoblast cells mimics the phenotype and differentiation of cytotrophoblasts from normal and preeclamptic pregnancies. *Exp Cell Res.* 2004;297(2):415-23.
71. Cheng Y, Zhao G, Zhang S, Nigim F, Zhou G, Yu Z, et al. AS1411-Induced Growth Inhibition of Glioma Cells by Up-Regulation of p53 and Down-Regulation of Bcl-2 and Akt1 via Nucleolin. *PLoS One.* 2016;11(12):e0167094.
72. Reyes-Reyes EM, Salipur FR, Shams M, Forsthoefel MK, and Bates PJ. Mechanistic studies of anticancer aptamer AS1411 reveal a novel role for nucleolin in regulating Rac1 activation. *Mol Oncol.* 2015;9(7):1392-405.

73. Kuo CW, Shiu JY, Chien FC, Tsai SM, Chueh DY, and Chen P. Polymeric nanopillar arrays for cell traction force measurements. *Electrophoresis.* 2010;31(18):3152-8.
74. Shiu JY, Aires L, Lin Z, and Vogel V. Nanopillar force measurements reveal actin-cap-mediated YAP mechanotransduction. *Nat Cell Biol.* 2018;20(3):262-71.
75. O'Sullivan T, Saddawi-Konefka R, Gross E, Tran M, Mayfield SP, Ikeda H, et al. Interleukin-17D mediates tumor rejection through recruitment of natural killer cells. *Cell Rep.* 2014;7(4):989-98.
76. Subramanian A, Tamayo P, Mootha VK, Mukherjee S, Ebert BL, Gillette MA, et al. Gene set enrichment analysis: a knowledge-based approach for interpreting genome-wide expression profiles. *Proc Natl Acad Sci U S A.* 2005;102(43):15545-50.
77. Reimand J, Isserlin R, Voisin V, Kucera M, Tannus-Lopes C, Rostamianfar A, et al. Pathway enrichment analysis and visualization of omics data using g:Profiler, GSEA, Cytoscape and EnrichmentMap. *Nature protocols.* 2019;14(2):482-517.
78. Wang Y, Yang C, Gu Q, Sims M, Gu W, Pfeffer LM, et al. KLF4 Promotes Angiogenesis by Activating VEGF Signaling in Human Retinal Microvascular Endothelial Cells. *PLoS One.* 2015;10(6):e0130341.
79. Liabotis A, Ardidie-Robouant C, Mailly P, Besbes S, Gutierrez C, Atlas Y, et al. Angiopoietin-like 4-Induced 3D Capillary Morphogenesis Correlates to Stabilization of Endothelial Adherens Junctions and Restriction of VEGF-Induced Sprouting. *Biomedicines.* 2022;10(2).
80. Thomas M, and Augustin HG. The role of the Angiopoietins in vascular morphogenesis. *Angiogenesis.* 2009;12(2):125-37.
81. Balaji Ragunathrao VA, Anwar M, Akhter MZ, Chavez A, Mao Y, Natarajan V, et al. Sphingosine-1-Phosphate Receptor 1 Activity Promotes Tumor Growth by Amplifying VEGF-VEGFR2 Angiogenic Signaling. *Cell Rep.* 2019;29(11):3472-87 e4.
82. DeWaal D, Nogueira V, Terry AR, Patra KC, Jeon SM, Guzman G, et al. Hexokinase-2 depletion inhibits glycolysis and induces oxidative phosphorylation in hepatocellular carcinoma and sensitizes to metformin. *Nat Commun.* 2018;9(1):446.
83. Lebherz HG, and Rutter WJ. Distribution of fructose diphosphate aldolase variants in biological systems. *Biochemistry.* 1969;8(1):109-21.
84. Vizin T, and Kos J. Gamma-enolase: a well-known tumour marker, with a less-known role in cancer. *Radiol Oncol.* 2015;49(3):217-26.
85. Feng Y, Zhang Y, Cai Y, Liu R, Lu M, Li T, et al. A20 targets PFKL and glycolysis to inhibit the progression of hepatocellular carcinoma. *Cell Death Dis.* 2020;11(2):89.
86. Lee JH, Liu R, Li J, Zhang C, Wang Y, Cai Q, et al. Stabilization of phosphofructokinase 1 platelet isoform by AKT promotes tumorigenesis. *Nat Commun.* 2017;8(1):949.
87. Eelen G, Cruys B, Welti J, De Bock K, and Carmeliet P. Control of vessel sprouting by genetic and metabolic determinants. *Trends Endocrinol Metab.* 2013;24(12):589-96.
88. De Bock K, Georgiadou M, Schoors S, Kuchnio A, Wong BW, Cantelmo AR, et al. Role of PFKFB3-driven glycolysis in vessel sprouting. *Cell.* 2013;154(3):651-63.
89. Rohlenova K, Veys K, Miranda-Santos I, De Bock K, and Carmeliet P. Endothelial Cell Metabolism in Health and Disease. *Trends Cell Biol.* 2018;28(3):224-36.
90. Cruys B, Wong BW, Kuchnio A, Verdegem D, Cantelmo AR, Conradi LC, et al. Glycolytic regulation of cell rearrangement in angiogenesis. *Nat Commun.* 2016;7:12240.
91. Paglia G, Williams JP, Menikarachchi L, Thompson JW, Tyldesley-Worster R, Halldorsson S, et al. Ion mobility derived collision cross sections to support metabolomics applications. *Anal Chem.* 2014;86(8):3985-93.
92. Ying W. NAD+/NADH and NADP+/NADPH in cellular functions and cell death: regulation and biological consequences. *Antioxid Redox Signal.* 2008;10(2):179-206.

93. Houtkooper RH, Canto C, Wanders RJ, and Auwerx J. The secret life of NAD+: an old metabolite controlling new metabolic signaling pathways. *Endocr Rev.* 2010;31(2):194-223.
94. Aragones J, Schneider M, Van Geyte K, Fraisl P, Dresselaers T, Mazzone M, et al. Deficiency or inhibition of oxygen sensor Phd1 induces hypoxia tolerance by reprogramming basal metabolism. *Nature genetics.* 2008;40(2):170-80.
95. Schoors S, Bruning U, Missiaen R, Queiroz KC, Borgers G, Elia I, et al. Fatty acid carbon is essential for dNTP synthesis in endothelial cells. *Nature.* 2015;520(7546):192-7.
96. Kalucka J, Bierhansl L, Conchinha NV, Missiaen R, Elia I, Bruning U, et al. Quiescent Endothelial Cells Upregulate Fatty Acid beta-Oxidation for Vasculoprotection via Redox Homeostasis. *Cell metabolism.* 2018;28(6):881-94 e13.
97. Mancuso MR, Kuhnert F, and Kuo CJ. Developmental angiogenesis of the central nervous system. *Lymphat Res Biol.* 2008;6(3-4):173-80.
98. Risau W. Mechanisms of angiogenesis. *Nature.* 1997;386(6626):671-4.
99. Galzio R, Rosati F, Benedetti E, Cristiano L, Aldi S, Mei S, et al. Glycosilated nucleolin as marker for human gliomas. *Journal of cellular biochemistry.* 2012;113(2):571-9.
100. Ghajar CM, Peinado H, Mori H, Matei IR, Evason KJ, Brazier H, et al. The perivascular niche regulates breast tumour dormancy. *Nat Cell Biol.* 2013;15(7):807-17.
101. Kuhnert F, Mancuso MR, Shamloo A, Wang HT, Choksi V, Florek M, et al. Essential regulation of CNS angiogenesis by the orphan G protein-coupled receptor GPR124. *Science.* 2010;330(6006):985-9.
102. Chang J, Mancuso MR, Maier C, Liang X, Yuki K, Yang L, et al. Gpr124 is essential for blood-brain barrier integrity in central nervous system disease. *Nat Med.* 2017;23(4):450-60.
103. Plate KH, Breier G, Weich HA, and Risau W. Vascular endothelial growth factor is a potential tumour angiogenesis factor in human gliomas in vivo. *Nature.* 1992;359(6398):845-8.
104. Cantelmo AR, Conradi LC, Brajic A, Goveia J, Kalucka J, Pircher A, et al. Inhibition of the Glycolytic Activator PFKFB3 in Endothelium Induces Tumor Vessel Normalization, Impairs Metastasis, and Improves Chemotherapy. *Cancer cell.* 2016;30(6):968-85.
105. Eelen G, de Zeeuw P, Simons M, and Carmeliet P. Endothelial cell metabolism in normal and diseased vasculature. *Circ Res.* 2015;116(7):1231-44.
106. Pitulescu ME, Schmidt I, Benedito R, and Adams RH. Inducible gene targeting in the neonatal vasculature and analysis of retinal angiogenesis in mice. *Nature protocols.* 2010;5(9):1518-34.
107. Veys K, Fan Z, Ghobrial M, Bouche A, Garcia-Caballero M, Vriens K, et al. Role of the GLUT1 Glucose Transporter in Postnatal CNS Angiogenesis and Blood-Brain Barrier Integrity. *Circ Res.* 2020;127(4):466-82.
108. De Bock K, Georgiadou M, and Carmeliet P. Role of endothelial cell metabolism in vessel sprouting. *Cell metabolism.* 2013;18(5):634-47.
109. Engelhardt S, Patkar S, and Ogunshola OO. Cell-specific blood-brain barrier regulation in health and disease: a focus on hypoxia. *British journal of pharmacology.* 2014;171(5):1210-30.
110. Argaw AT, Zhang Y, Snyder BJ, Zhao ML, Kopp N, Lee SC, et al. IL-1beta regulates blood-brain barrier permeability via reactivation of the hypoxia-angiogenesis program. *J Immunol.* 2006;177(8):5574-84.
111. Quail DF, and Joyce JA. The Microenvironmental Landscape of Brain Tumors. *Cancer cell.* 2017;31(3):326-41.
112. Batchelor TT, Gerstner ER, Emblem KE, Duda DG, Kalpathy-Cramer J, Snuderl M, et al. Improved tumor oxygenation and survival in glioblastoma patients who show increased

blood perfusion after cediranib and chemoradiation. *Proc Natl Acad Sci U S A.* 2013;110(47):19059-64.

113. Emblem KE, Mouridsen K, Bjornerud A, Farrar CT, Jennings D, Borra RJ, et al. Vessel architectural imaging identifies cancer patient responders to anti-angiogenic therapy. *Nat Med.* 2013;19(9):1178-83.

FIGURE LEGENDS

Figure 1

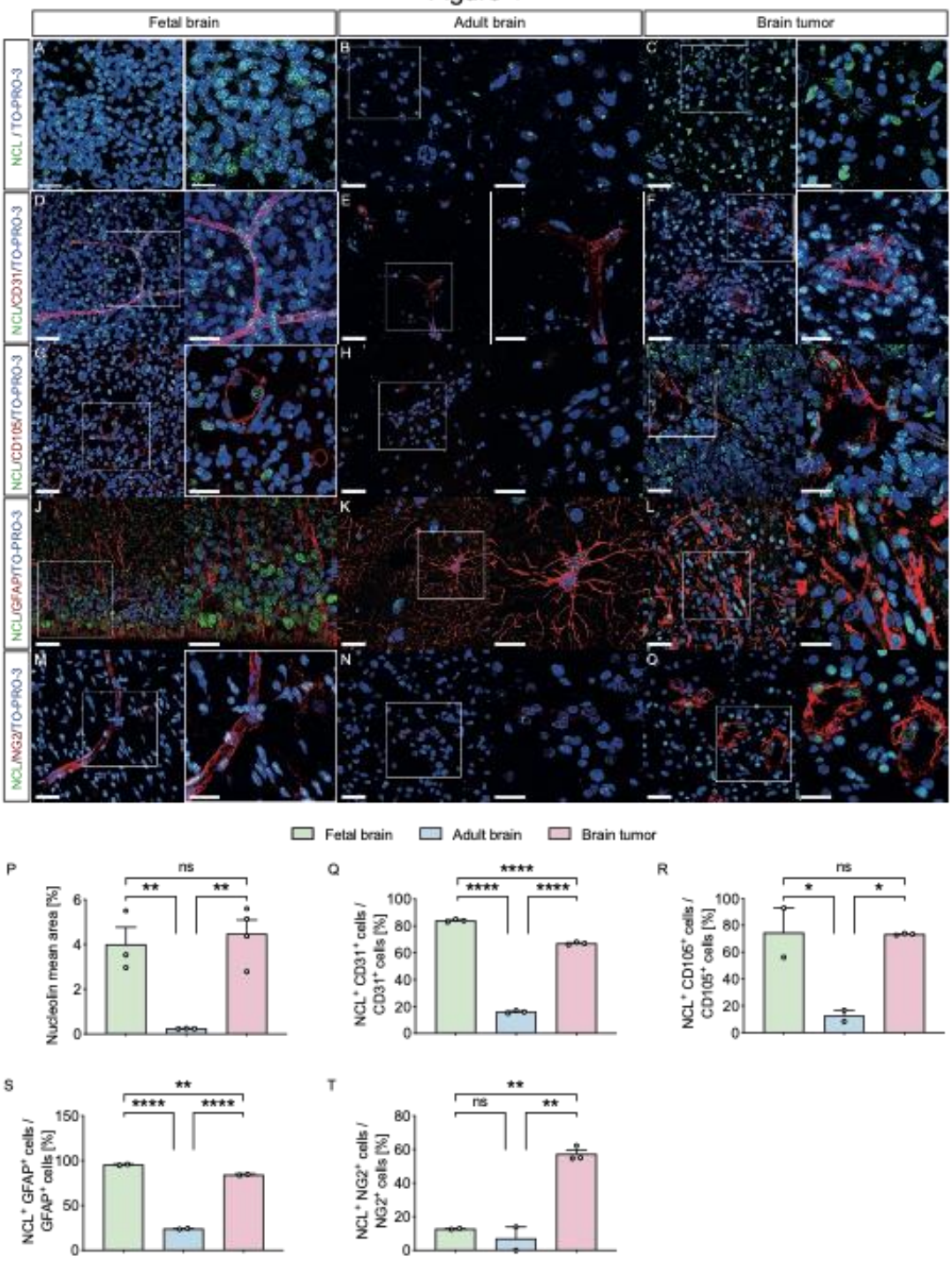
Fetal brain
Adult brain
Brain tumor
NCL / TO-PRO-3
NCL/CD31/TO-PRO-3
NCL/CD105/TO-PRO-3
NCL/GFAP/TO-PRO-3
NCL/NG2/TO-PRO-3
A
B
C
D
E
F
G
H
J
K
L
M
N
O
Fetal brain
Adult brain
Brain tumor
P
Nucleolin mean area [%]
ns
**
**
Q
NCL+ CD31+ cells / CD31+ cells [%]
****
****
****
R
NCL+ CD105+ cells / CD105+ cells [%]
ns
*
*
S
NCL+ GFAP+ cells / GFAP+ cells [%]
**
****
****
T
NCL+ NG2+ cells / NG2+ cells [%]
**
ns
**

Figure 1 Nucleolin is expressed in endothelial- and perivascular cells during human brain development, is downregulated in the adult brain, and is reactivated in glial brain tumors in vivo

20 µm sections of human fetal- (GW 18-22) and adult brains as well as from human GBMs were stained for Nucleolin, the vascular endothelial cell markers CD31 and CD105, the astrocytic marker GFAP, the pericyte marker NG2, and TO-PRO-3 nuclear counterstaining.

A-C,**P** Nucleolin (green) is highly expressed in the nuclei of the developing human fetal brain (**A**) and of human brain tumors (**C**), but shows a significant downregulation in the adult normal/healthy brain (**B**,**P**).

D-I,**Q**,**R** Nucleolin (green) is highly expressed in $CD31^+$ blood vessel endothelial cells (red) in the human fetal (**D**,**Q**)- and pathological brain (**F**,**Q**), but is significantly downregulated in endothelial cell of the quiescent adult brain (**E**,**Q**). Nucleolin shows a high expression in $CD105^+$activated endothelial cells (red) in the human fetal brain (**G**,**R**) and in glioblastoma (**I**,**R**) but is significantly downregulated in the quiescent adult normal brain (**H**,**R**), with a very low number of $CD105^+$ endothelial cells in the quiescent adult brain (**H**,**R**).

J-L,**S** Nucleolin (green) is highly expressed in $GFAP^+$ neural precursors cells (red) in the fetal brain (**J**) and in tumoral astrocytes in glioblastoma (**L**) but is significantly downregulated in adult normal brain (**K**,**S**).

M-O,**T** In human fetal and adult brains, $NG2^+$ pericytes (red) partially express low levels of Nucleolin (**M**,**N**). Nucleolin expression is highly upregulated in human brain tumor $NG2^+$ pericytes (**O**,**T**).

Data represent mean ± SEM of 2-3 patients (2-3 sections per patient, based on tissue availability). For statistical analysis, one-way ANOVAs with Tukey's post-hoc test were performed. $*P < 0.05$, $**P < 0.01$, $****P < 0.0001$. Scale bars: 25 µm in **A-O**, **left panels**; and 15 µm in **A-O**, **right panels**.

Figure 2

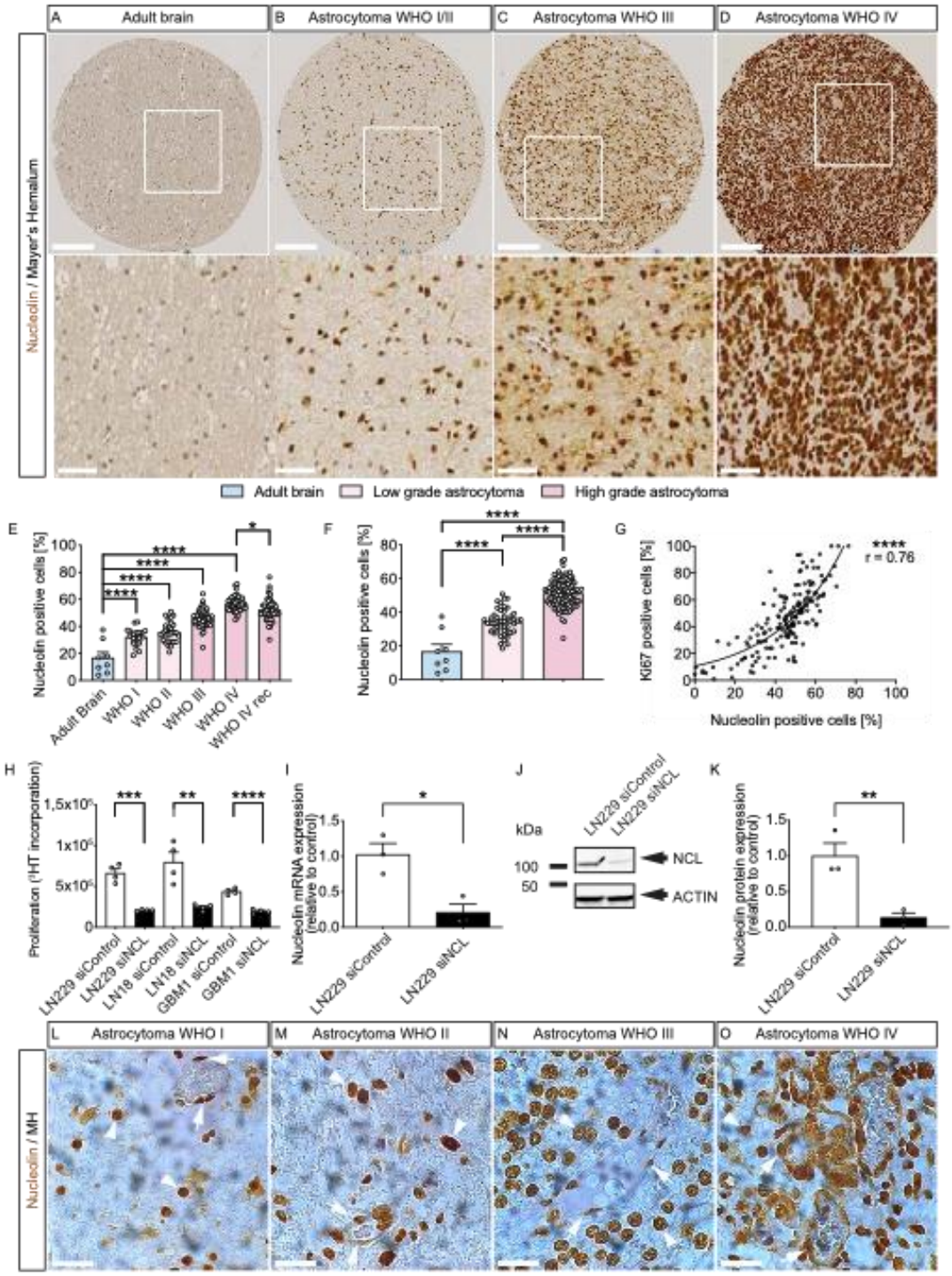
A Adult brain
B Astrocytoma WHO I/II
C Astrocytoma WHO III
D Astrocytoma WHO IV
Nucleolin / Mayer's Hemalaun
Adult brain
Low grade astrocytoma
High grade astrocytoma
E
Nucleolin positive cells [%]
Adult Brain
WHO I
WHO II
WHO III
WHO IV
WHO IV rec
F
Nucleolin positive cells [%]
G
Ki67 positive cells [%]
Nucleolin positive cells [%]
r = 0.76
H
Proliferation (³HT incorporation)
LN229 siControl
LN229 siNCL
LN18 siControl
LN18 siNCL
GBM1 siControl
GBM1 siNCL
I
Nucleolin mRNA expression (relative to control)
LN229 siControl
LN229 siNCL
J
kDa
LN229 siControl
LN229 siNCL
100
50
NCL
ACTIN
K
Nucleolin protein expression (relative to control)
LN229 siControl
LN229 siNCL
L Astrocytoma WHO I
M Astrocytoma WHO II
N Astrocytoma WHO III
O Astrocytoma WHO IV
Nucleolin / MH

Figure 2 Expression of Nucleolin increases during astrocytic tumor progression and Nucleolin is expressed in blood vessels in low- and high-grade gliomas in vivo

A-F Nucleolin (brown) expression increases during tumor progression of human astrocytomas from WHO grade I (**A**, n=20), II (**B**, n=28), III (**C**, n=53) to IV (= glioblastoma, **D**, n=46). In low-grade astrocytomas (WHO grades I and II, n=48), Nucleolin expression is significantly higher than in the normal brain parenchyma (**E,F**, n=8), but significantly lower as compared to high-grade astrocytomas (**E**,**F**, WHO grades III and IV, n=96). Nucleolin expression slightly decreases in recurrent WHO grade IV tumors (**E,** n=49).

G Nucleolin expression positively correlates with the expression of the proliferation marker Ki-67 in gliomas (n=167).

H Glioblastoma cell lines (LN229, LN18 and GBM-1) proliferation was significantly decreased upon Nucleolin knock-down (n=4).

I Quantitative RT-PCR revealing a significant downregulation of about 70% of Nucleolin mRNA expression upon siRNA-targeted Nucleolin knock down (siNCL, n=3).

J Western blot showing Nucleolin downregulation in LN229 cells transfected with siRNA against Nucleolin (siNCL) (n=3). No Nucleolin downregulation was observed in LN229 transfected with the control siRNA (siControl) (n=3).

K Quantification of Western blot revealing a significant downregulation of Nucleolin protein expression by siRNA-targeted Nucleolin knock down as compared to control cells in LN-229 cells (n=3).

L-O Nucleolin expression in tumor blood vessels. Note the increasing expression of Nucleolin in the blood vessel wall (arrows) as well as in perivascular cells (arrowheads) in astrocytomas of higher grades.

Data represent mean ± SEM. For statistical analysis, one-way ANOVA with Tukey's post-hoc test (**E**,**F**), Pearson correlation analysis (**G**) and two-tailed unpaired Student's t -test (**H**,**I**,**K**) were

performed. $^{**}P < 0.01$, $^{****}P < 0.0001$. Scale bars: 100 μm (**A**-**D**, upper panel), 50 μm (**A**-**D**, lower panel, and **G**-**J**).

Figure 3

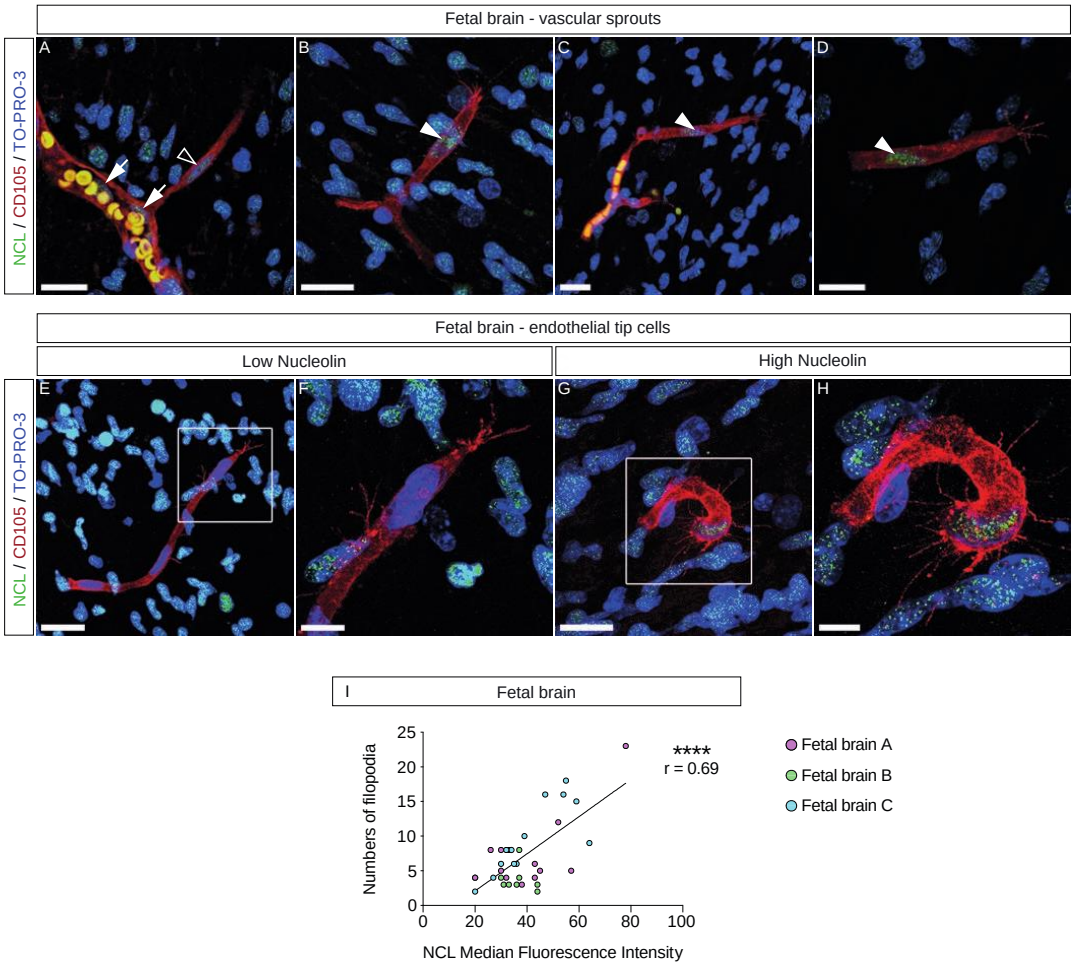
Fetal brain - vascular sprouts
NCL / CD105 / TO-PRO-3
A
B
C
D
Fetal brain - endothelial tip cells
Low Nucleolin
High Nucleolin
NCL / CD105 / TO-PRO-3
E
F
G
H

I
Fetal brain
Numbers of filopodia
NCL Median Fluorescence Intensity
****
r = 0.69
Fetal brain A
Fetal brain B
Fetal brain C

Figure 3 Nucleolin is expressed in endothelial tip-, stalk-, and phalanx cells of vascular sprouts and Nucleolin expression correlates with the number of endothelial tip cell filopodia in the human fetal brain in vivo

A-**D** $CD105^{+}$ blood vessel sprouts (red) in the human fetal brain grow in CNS tissue with vascular- and parenchymal expression of Nucleolin, respectively. Nucleolin (green) is expressed in endothelial tip (filled arrowheads in **B**,**C**,**D**)- stalk (empty arrowhead in **A**)- and phalanx cells (plain arrows in **A**) in growing vessels in the human fetal (GW18-22) cortex.

E-H Vascular sprouts with CD105-labeled endothelial tip cells (red) with low- (**E**,**F**) and high (**G**,**H**) Nucleolin (green) expression in the human fetal cortex.

Numerous filopodial protrusions emerged from the endothelial tip cell body with high Nucleolin expression (**G**,**H**) as compared to only few filopodial protrusions in an endothelial tip cell with low Nucleolin expression (**E**,**F**). (**I**) The number of filopodia per endothelial tip cell strongly correlated with the intensity of Nucleolin expression in the respective endothelial tip cell. Each dot represents an endothelial tip cell with its median NCL expression and number of filopodia(n=35). Dots are colored by patients (n=3 patients, 2-3 sections per patient, based on tissue availability).

For statistical analysis, Pearson correlation analysis (**I**) was performed. ****$P < 0.0001$. Scale bars: 20 μm in **A**-**D**; 25 μm in **E** and **G**; and 10 μm in **F** and **H**.

Figure 4

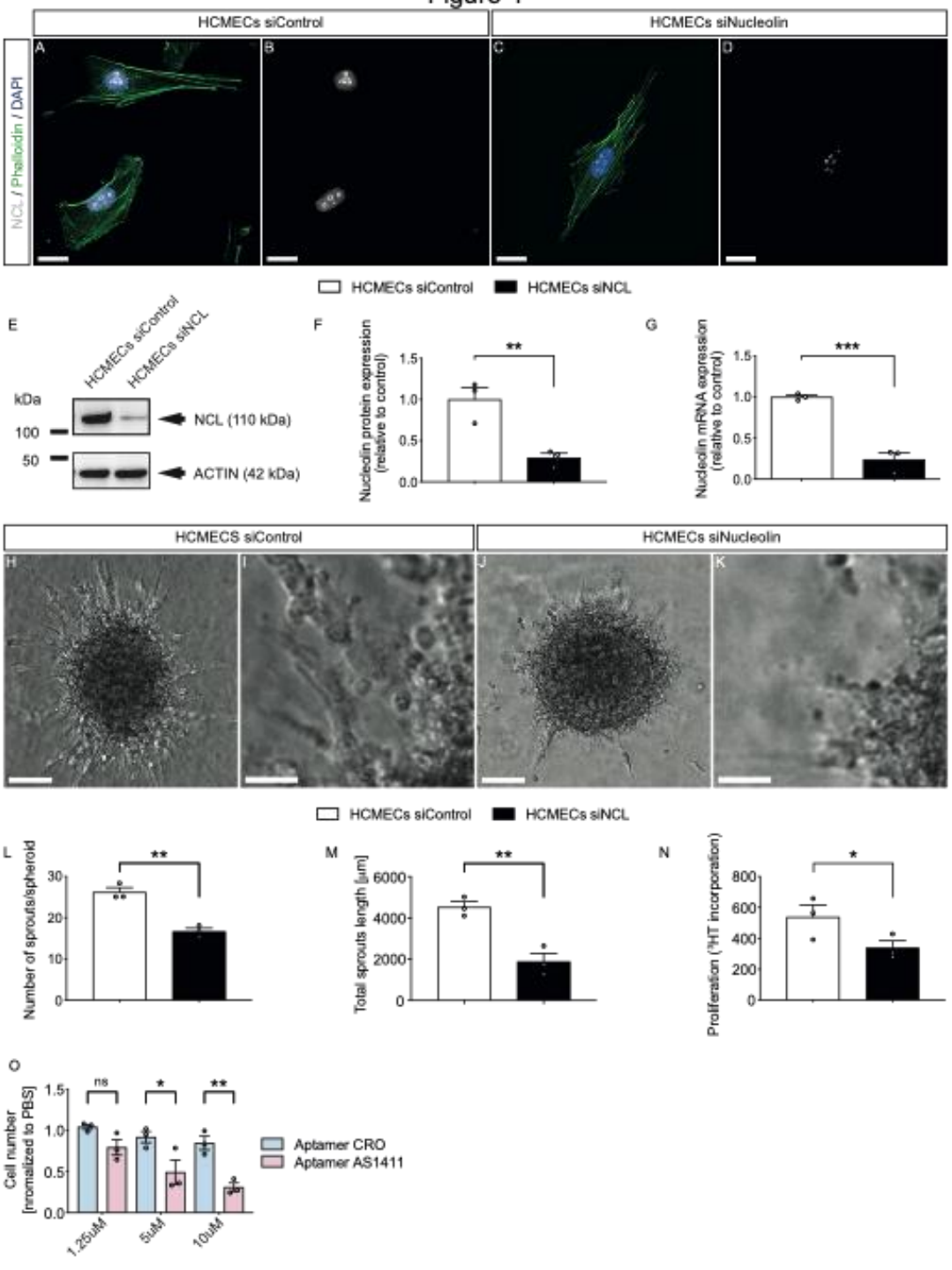
HCMECs siControl
HCMECs siNucleolin
NCL / Phalloidin / DAPI
A
B
C
D
HCMECs siControl
HCMECs siNCL
E
HCMECs siControl
HCMECs siNCL
kDa
100
50
NCL (110 kDa)
ACTIN (42 kDa)
F
Nucleolin protein expression (relative to control)
**
G
Nucleolin mRNA expression (relative to control)
***
HCMECS siControl
HCMECs siNucleolin
H
I
J
K
HCMECs siControl
HCMECs siNCL
L
Number of sprouts/spheroid
**
M
Total sprouts length [µm]
**
N
Proliferation (³HT incorporation)
*
O
Cell number [normalized to PBS]
ns
*
**
1.25uM
5uM
10uM
Aptamer CRO
Aptamer AS1411

Figure 4 Nucleolin promotes brain vascular endothelial cell sprouting and proliferation in vitro and can be targeted with the Nucleolin-specific aptamer AS1411

A-**D** HCMECs were stained for Nucleolin (green), F-actin (stained with Phalloidin, red), and the general nuclear marker DAPI (blue). Nucleolin expression was decreased and restricted to nucleoli upon siRNA-mediated knockdown in HCMECs (**C**,**D**) as compared to control-siRNA treated HCMECs (**A**,**B**).

E Western blot showing Nucleolin downregulation in HCMECs transfected with siRNA against Nucleolin (siNCL) as compared to control-siRNA treated HCMECs (n=3).

F Quantification of Western blot revealing a significant downregulation of 70% Nucleolin protein expression by siRNA-targeted Nucleolin knock down as compared to control cells (n=3).

G Quantitative RT-PCR revealing a significant downregulation of more than 80% of Nucleolin mRNA expression by siRNA-targeted Nucleolin knock down (n=3).

H-**K** HCMEC sprout formation (number of sprouts per spheroid) was decreased upon siRNA-mediated Nucleolin knockdown (**J**,**K**) as compared to the control group (**H**,**I**). The boxed areas in **H**,**J** are enlarged in **I**,**K** respectively.

L,**M** HCMEC sprout formation and total sprout length were significantly reduced upon Nucleolin knock-down as compared to the control group (**L**,**M**) (n=3).

N HCMEC proliferation was significantly decreased upon Nucleolin knock down (n=3).

O HCMEC cell proliferation was dose-dependently decreased upon treatment with the Nucleolin-specific aptamer AS1411. Cells were treated for 96h with 1.25uM, 5uM and 10uM of the Nucleolin targeting aptamer AS1411 or the control aptamer CRO, respectively (n=3).

Data represent mean ± SEM. For statistical analysis, two-tailed unpaired Student's t -test (**F**-**G**, **L**-**N**) and two-way ANOVA with Tukey's multiple comparison test with Tukey's multiple-comparison test comparing treatment columns (**O**) were performed. **P* < 0.05, ***P* < 0.01, ****P* < 0.001, *****P* < 0.0001. Scale bars: 20 µm in **A**-**D**; 150 µm in **H** and **J**; and 50 µm in **I** and**K**.

Figure 5

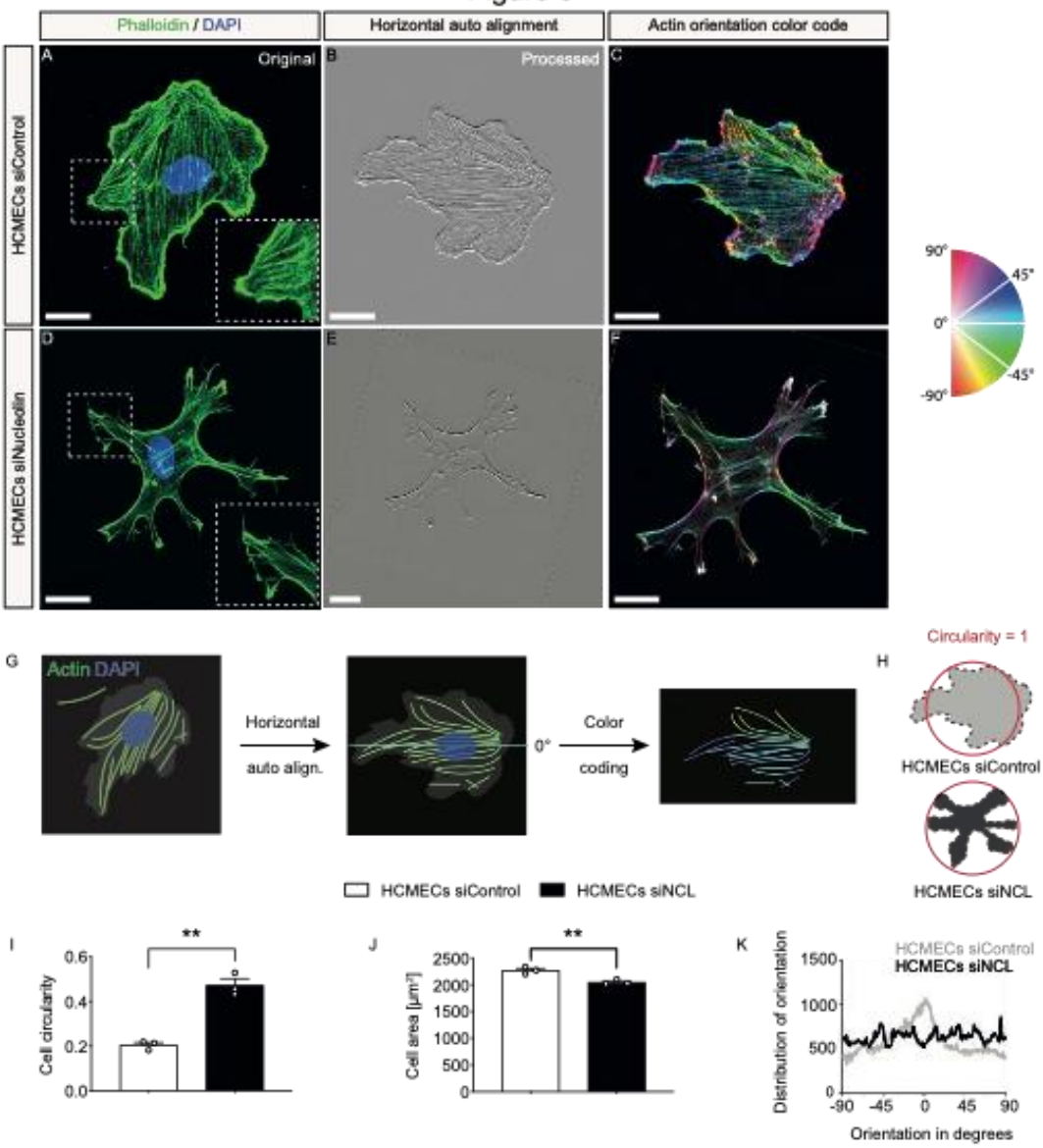
Phalloidin / DAPI
Horizontal auto alignment
Actin orientation color code
HCMECs siControl
HCMECs siNucleolin
A
Original
B
Processed
C
D
E
F
90°
45°
0°
-45°
-90°
G
Actin DAPI
Horizontal
auto align.
0°
Color
coding
H
Circularity = 1
HCMECs siControl
HCMECs siNCL
HCMECs siControl
HCMECs siNCL
I
**
Cell circularity
0.6
0.4
0.2
0.0
J
**
Cell area [µm²]
2500
2000
1500
1000
500
0
K
HCMECs siControl
HCMECs siNCL
Distribution of orientation
1500
1000
500
0
-90
-45
0
45
90
Orientation in degrees

Figure 5 Nucleolin affects HCMEC actin cytoskeleton orientation in vitro

A-F HCMEC treated with control- or Nucleolin siRNA were left to spread on fibronectin-coated glass substrate and stained for F-actin (green) and DAPI (blue) (**A,D**).

G Scheme illustrating actin fiber orientation characterization.

H Schematic illustration of circularity index indicating the reference circular index (circle = 1).

I,**J** Nucleolin knockdown decreased HCMEC cell spreading, as measured by cell circularity and cell area measurements. Nucleolin knock down HCMECs had a significantly less elongated shape(**I**, n=3). HCMEC spreading was significantly decreased upon Nucleolin knockdown (**J**, n=3).

K Phalloidin actin fibers (green) were more randomly organized in the $HCMEC^{Nucleolin\ KD}$ (**E**,**F**) as compared to the control (**B**,**C**). The distribution of actin orientation shows clear classical peak close to 0 degree in the control $HCMEC^{Control\ KD}$ (grey curve). In $HCMEC^{Nucleolin\ KD}$, the classical peak of actin orientation was lost and HCMEC actin orientation was more randomly distributed (black curve) (**K**).

Data represent mean ± SEM. For statistical analysis, two-tailed unpaired Student's t -test were performed. $*P < 0.05$, $**P < 0.01$, $***P < 0.001$. Scale bars: 20 µm in A-F.

Figure 6

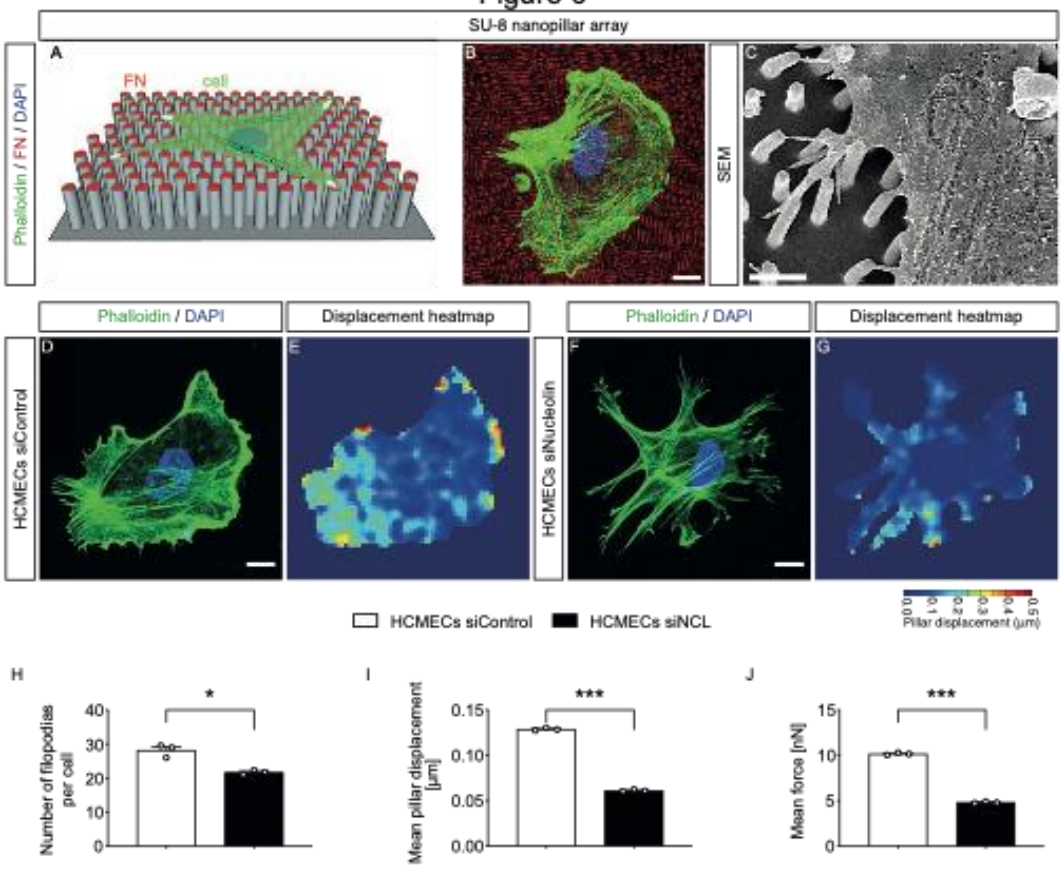
SU-8 nanopillar array
A
FN
cell
Phalloidin / FN / DAPI
B
C
SEM
Phalloidin / DAPI
Displacement heatmap
Phalloidin / DAPI
Displacement heatmap
HCMECs siControl
D
E
HCMECs siNucleolin
F
G
0.0
0.1
0.2
0.3
0.4
0.5
Pillar displacement (µm)
HCMECs siControl
HCMECs siNCL
H
Number of filopodias per cell
40
30
20
10
0
*
I
Mean pillar displacement [µm]
0.15
0.10
0.05
0.00
***
J
Mean force [nN]
15
10
5
0
***

Figure 6 Nucleolin regulates HCMEC lamellipodia and filopodia in vitro

A-**C** Scheme illustrating a spread endothelial cell (green) on a SU-8 nanopillar array (grey) coated with fibronectin (red) (**A**). F-actin (green) and DAPI (blue) stained HCMEC on a fibronectin-coated nanopillar substrate (red) (**B**). Scanning electron microscopy (SEM) image of HCMEC filopodia attaching to nanopillars (**C**). Note the nanopillar-deflection caused by retracting HCMEC filopodia (arrowheads), allowing to optically measure the displacement of the nanopillar and the induced corresponding traction forces.

D-**J** HCMECs treated with siRNA (for Nucleolin, and control) were placed on nanopillar substrates, and were stained for F-actin (green) and the general nuclear marker DAPI (blue) (**D**,**F**). The number of filopodia per cell was decreased significantly in siRNA-mediated Nucleolin knockdown in comparison with control siRNA-treated HCMECs (**H**, n=3). Explorative movements of HCMECs (and its lamellipodia- and filopodia extensions) were reduced upon Nucleolin knockdown as evidenced by displacement heatmaps (**E**,**G**, n=3). Nucleolin downregulation decreased mean nanopillar displacement (**I**) and mean filopodia force (**J**) accordingly.

Data represent mean ± SEM. For statistical analysis, two-tailed unpaired Student's t -test were performed. $*P < 0.05$, $**P < 0.01$, $***P < 0.001$. Scale bars: 10 µm in **B**; 2 µm in **C**; and 5 µm in **D**-**G**.

Figure 7

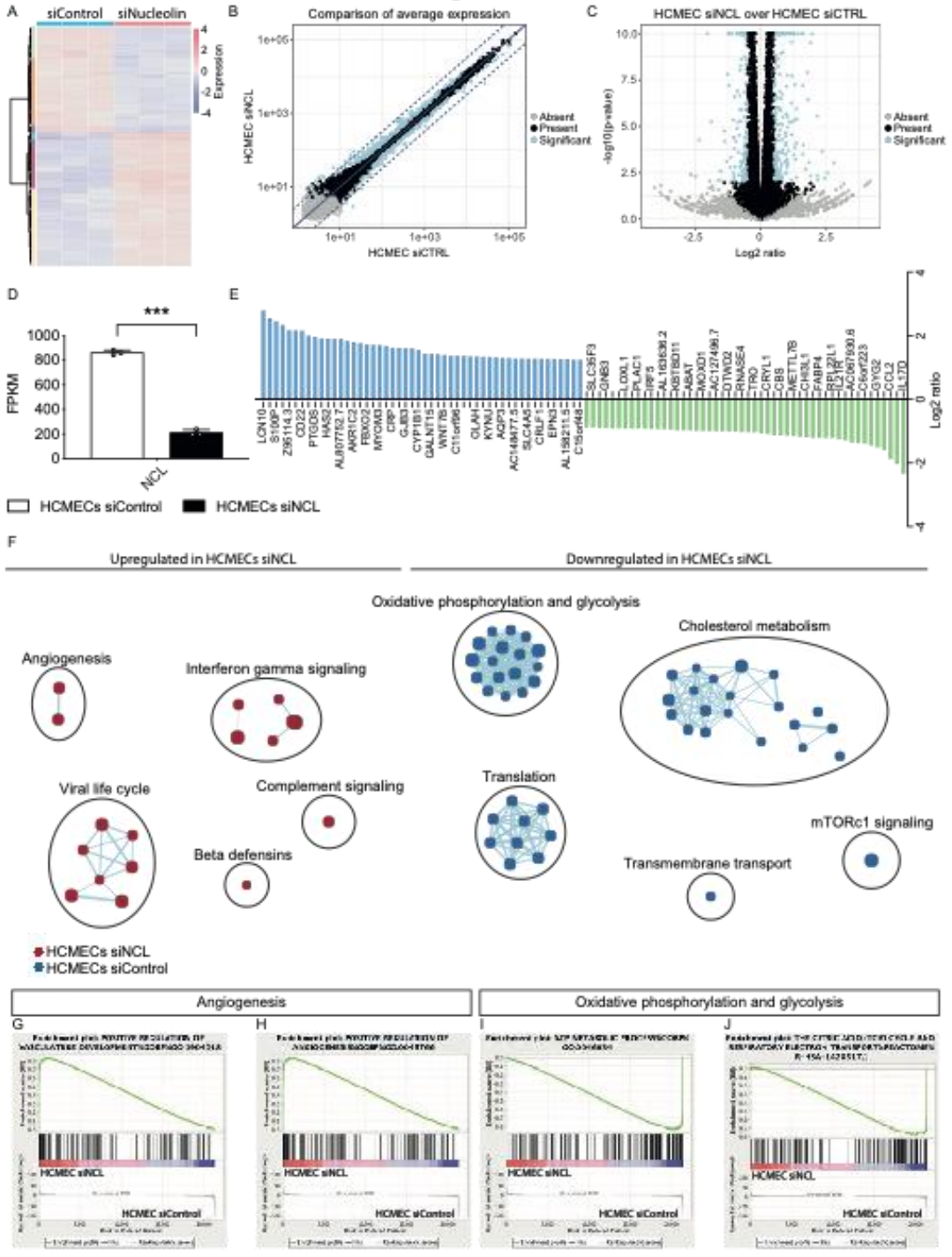
A
siControl
siNucleolin
Expression
B
Comparison of average expression
HCMEC siNCL
HCMEC siCTRL
Absent
Present
Significant
C
HCMEC siNCL over HCMEC siCTRL
-log10(p-value)
Log2 ratio
D
FPKM
***
NCL
HCMECs siControl
HCMECs siNCL
E
Log2 ratio
F
Upregulated in HCMECs siNCL
Downregulated in HCMECs siNCL
Angiogenesis
Interferon gamma signaling
Oxidative phosphorylation and glycolysis
Cholesterol metabolism
Viral life cycle
Complement signaling
Translation
mTORc1 signaling
Beta defensins
Transmembrane transport
HCMECs siNCL
HCMECs siControl
Angiogenesis
Oxidative phosphorylation and glycolysis
G
H
I
J
HCMEC siNCL
HCMEC siControl

Figure 7: Nucleolin induces regulation of angiogenic pathways including Dll4-Jagged-Notch-Hey-Hes-, YAP-TAZ-CTGF-Cyr61-, VEGF-A-VEGFR2 and endothelial glucose metabolism in HCMECs

Transcriptome analysis via RNA sequencing of HCMECs treated with small interfering RNA (siRNA) against Nucleolin (siNCL) and control siRNA (siControl) in three independent experiments.

A Heatmap and hierarchical clustering of siNucleolin treated HCMECs as compared to siControl treated HCMECs.

B,**C** 445 genes were differentially regulated between $HCMECs^{Nucleolin\ KD}$ and $HCMECs^{Control\ KD}$, and indicated in blue on scatter (**B**) and volcano plots (**C**).

D Nucleolin gene expression (FPKM) was significantly downregulated by siNucleolin treatment.

E Top 50 significantly up (blue)- or down (green)-regulated genes detected by RNA-seq in HCMECs upon Nucleolin knock down as compared to control treatment. Differentially regulated genes were arranged according to fold change of gene expression.

F-**J** Gene set enrichment analysis (GSEA), cytoscape enrichment map (**F**), and enrichment plots showed a significant up-regulation of signaling pathways related to regulation of angiogenesis (**F**-**H**) in HCMECs treated with siRNA against Nucleolin. Whereas pathways involved in metabolic processes such as oxidative phosphorylation and glycolysis (**F**,**I**,**J**) and cholesterol metabolism were enriched in the control treatment. Pathways enriched in Nucleolin KD HCMECs are labeled in red and pathways enriched in control HCMECs are labeled in blue. Pathways are indicated by colored nodes. Their size represents the number of genes they contain. Green lines indicate relationships between the pathways. Black circles group related pathways.

Data represent mean ± SEM. For statistical analysis, Wald tests corrected for multiple testing using the Benjamini and Hochberg method were performed.

Figure 8

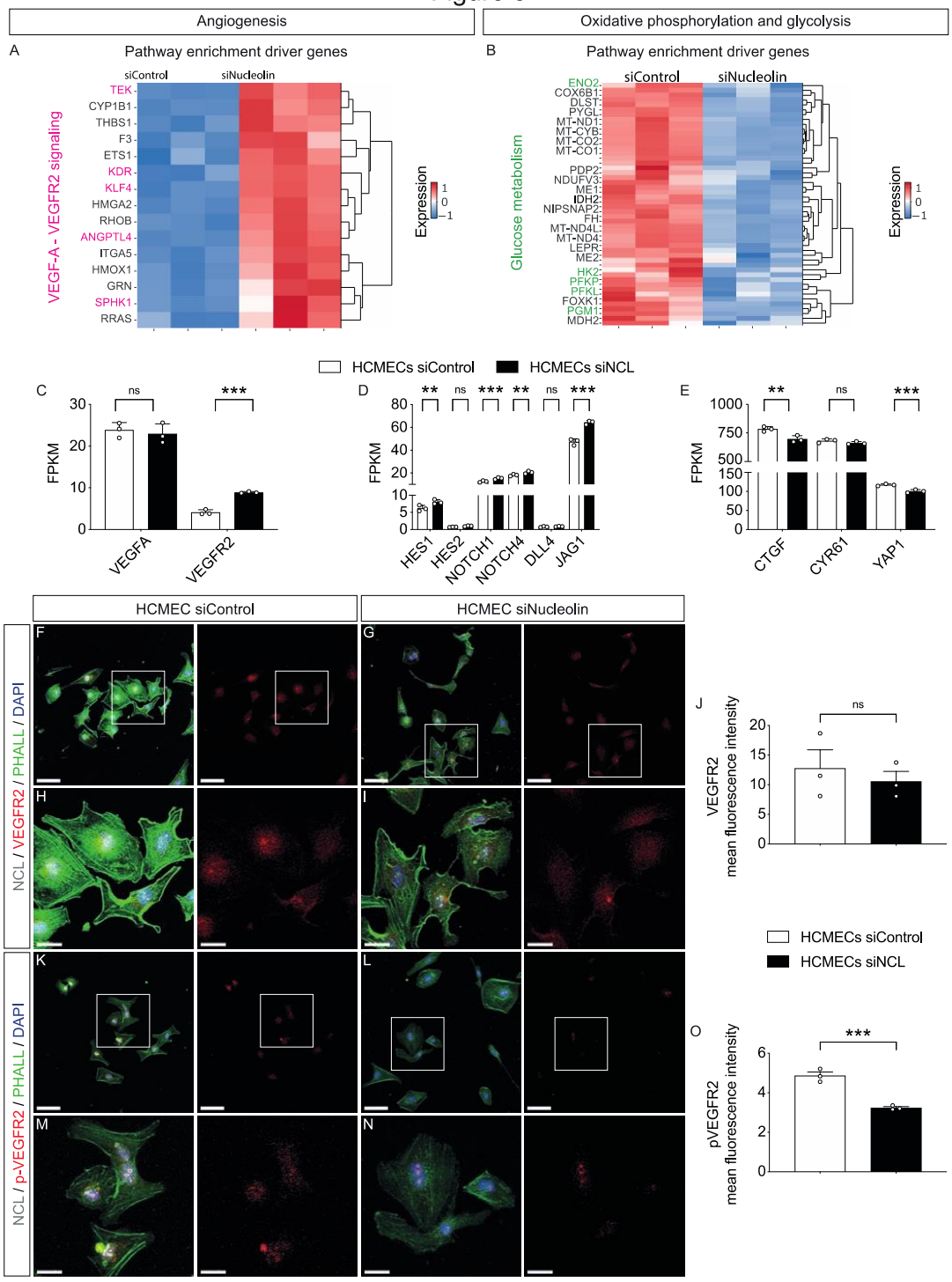
Angiogenesis
Oxidative phosphorylation and glycolysis
A
Pathway enrichment driver genes
siControl
siNucleolin
VEGF-A - VEGFR2 signaling
TEK
CYP1B1
THBS1
F3
ETS1
KDR
KLF4
HMGA2
RHOB
ANGPTL4
ITGA5
HMOX1
GRN
SPHK1
RRAS
Expression
B
Pathway enrichment driver genes
siControl
siNucleolin
Glucose metabolism
ENO2
COX6B1
DLST
PYGL
MT-ND1
MT-CYB
MT-CO2
MT-CO1
PDP2
NDUFV3
ME1
IDH2
NIPSNAP2
FH
MT-ND4L
MT-ND4
LEPR
ME2
HK2
PFKP
PFKL
FOXK1
PGM1
MDH2
Expression
HCMECs siControl
HCMECs siNCL
C
FPKM
ns
***
VEGFA
VEGFR2
D
FPKM
**
ns
***
**
ns
***
HES1
HES2
NOTCH1
NOTCH4
DLL4
JAG1
E
FPKM
**
ns
***
CTGF
CYR61
YAP1
HCMEC siControl
HCMEC siNucleolin
NCL / VEGFR2 / PHALL / DAPI
NCL / p-VEGFR2 / PHALL / DAPI
F
G
H
I
K
L
M
N
J
VEGFR2 mean fluorescence intensity
ns
HCMECs siControl
HCMECs siNCL
O
pVEGFR2 mean fluorescence intensity
***

Figure 8: Nucleolin induces regulation of angiogenic pathways and promotes phosphorylation of VEGFR2 in HCMECs

A,**B** Heatmap showing the expression of the top 15 genes driving the enrichment of "angiogenesis" pathways in $HCMEC^{Nucleolin\ KD}$ and the top 50 genes driving the enrichment of "oxidative phosphorylation and glycolysis" pathways in $HCMEC^{Control\ KD}$.

C-**E** *VEGFA* expression was not differentially regulated and *VEGFR2* expression was upregulated (**C**) in $HCMECs^{Nucleolin\ KD}$ as compared to $HCMECs^{Control\ KD}$ Nucleolin knock down induced a significant upregulation of the Dll4-Jagged-Notch signaling pathway including: *HES1*, *NOTCH1*, *NOTCH4*, Jagged1 (*JAG1*), while HES2 and DLL4 were not differentially regulated upon Nucleolin knock down (**D**). siNucleolin treatment caused a significant down-regulation of the YAP-TAZ gene *YAP1* as well as the YAP-TAZ downstream effector gene *CTGF* but not of the YAP-TAZ downstream effector gene *CYR61* (**E**).

F-**O** HCMECs were stained for Nucleolin (gray), F-actin (green, stained with Phalloidin), VEGFR2 (red, in **F**-**I**) or phopho-VEGFR2 (red, in **K**-**N**) and the general nuclear marker DAPI (blue). VEGFR2 expression was not regulated (**J**, n=3) but phospho-VEGFR2 expression was significantly downregulated (**O**, n=3) upon siRNA-mediated Nucleolin knockdown in HCMECs as compared to the control condition.

Data represent mean ± SEM. For statistical analysis, Wald test corrected for multiple testing using the Benjamini and Hochberg method (**C**-**E**) and two-tailed unpaired Student's t -test (**J**,**O**) were performed. $*P < 0.05$, $**P < 0.01$, $***P < 0.001$, $****P < 0.0001$. The boxed areas (white box) in **F**,**G**,**K**,**L** are zoomed in **H**,**I**,**M**,**N** respectively. Scale bars: 70 µm in **F**,**G**,**K**,**L**; and 20 µm in **H**,**I**,**M**,**N**.

Figure 9

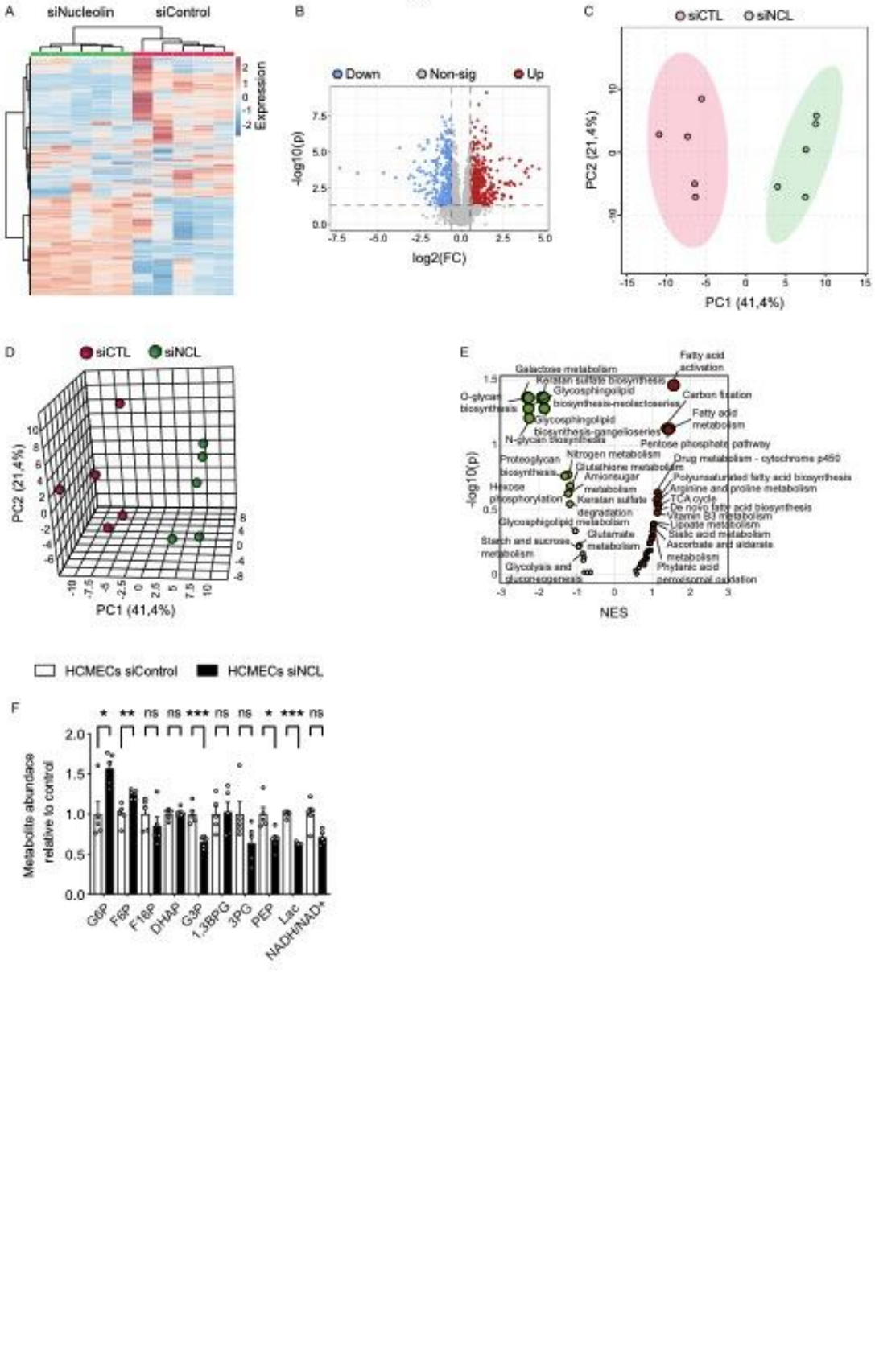
A
siNucleolin
siControl
Expression
B
Down
Non-sig
Up
-log10(p)
log2(FC)
C
siCTL
siNCL
PC2 (21,4%)
PC1 (41,4%)
D
siCTL
siNCL
PC2 (21,4%)
PC1 (41,4%)
E
Fatty acid activation
Galactose metabolism
Keratan sulfate biosynthesis
Glycosphingolipid biosynthesis-neolactoseries
O-glycan biosynthesis
Carbon fixation
Fatty acid metabolism
Glycosphingolipid biosynthesis-ganglioseries
N-glycan biosynthesis
Pentose phosphate pathway
Proteoglycan biosynthesis
Nitrogen metabolism
Drug metabolism - cytochrome p450
Glutathione metabolism
Aminosugar metabolism
Polyunsaturated fatty acid biosynthesis
Arginine and proline metabolism
Hexose phosphorylation
Keratan sulfate degradation
TCA cycle
De novo fatty acid biosynthesis
Vitamin B3 metabolism
Glycosphigolipid metabolism
Lipoate metabolism
Sialic acid metabolism
Glutamate metabolism
Starch and sucrose metabolism
Ascorbate and aldarate metabolism
Glycolysis and gluconeogenesis
Phytanic acid peroxisomal oxidation
-log10(p)
NES
HCMECs siControl
HCMECs siNCL
F
Metabolite abundace relative to control
G6P
F6P
F1BP
DHAP
G3P
1,3BPG
3PG
PEP
Lac
NADH/NAD+

Figure 9: Nucleolin regulates endothelial metabolism and alters metabolite profiles in human brain endothelial cells

A-F Metabolite profile comparison between siRNA Nucleolin KD HCMECs and control KD HCMECs (n=5). Heatmap and hierarchical clustering showing 2000 differentially regulated metabolites (**A**). Scatter plot showing the significantly regulated metabolites upon Nucleolin KD. 455 metabolites were significantly upregulated in $HCMECs^{Nucleolin\ KD}$ (indicated in red) and 292 metabolites were significantly downregulated (indicated in blue) (**B**). Two-dimensional and three-dimensional PCA plot of log-transformed normalized concentration of 2000 metabolites, each represent a sample, and colored by experimental group (**C**,**D**).

Data represent mean ± SEM. For statistical analysis, two-tailed unpaired Student's t -test were performed. $*P < 0.05$, $**P < 0.01$, $***P < 0.001$.

Figure 10

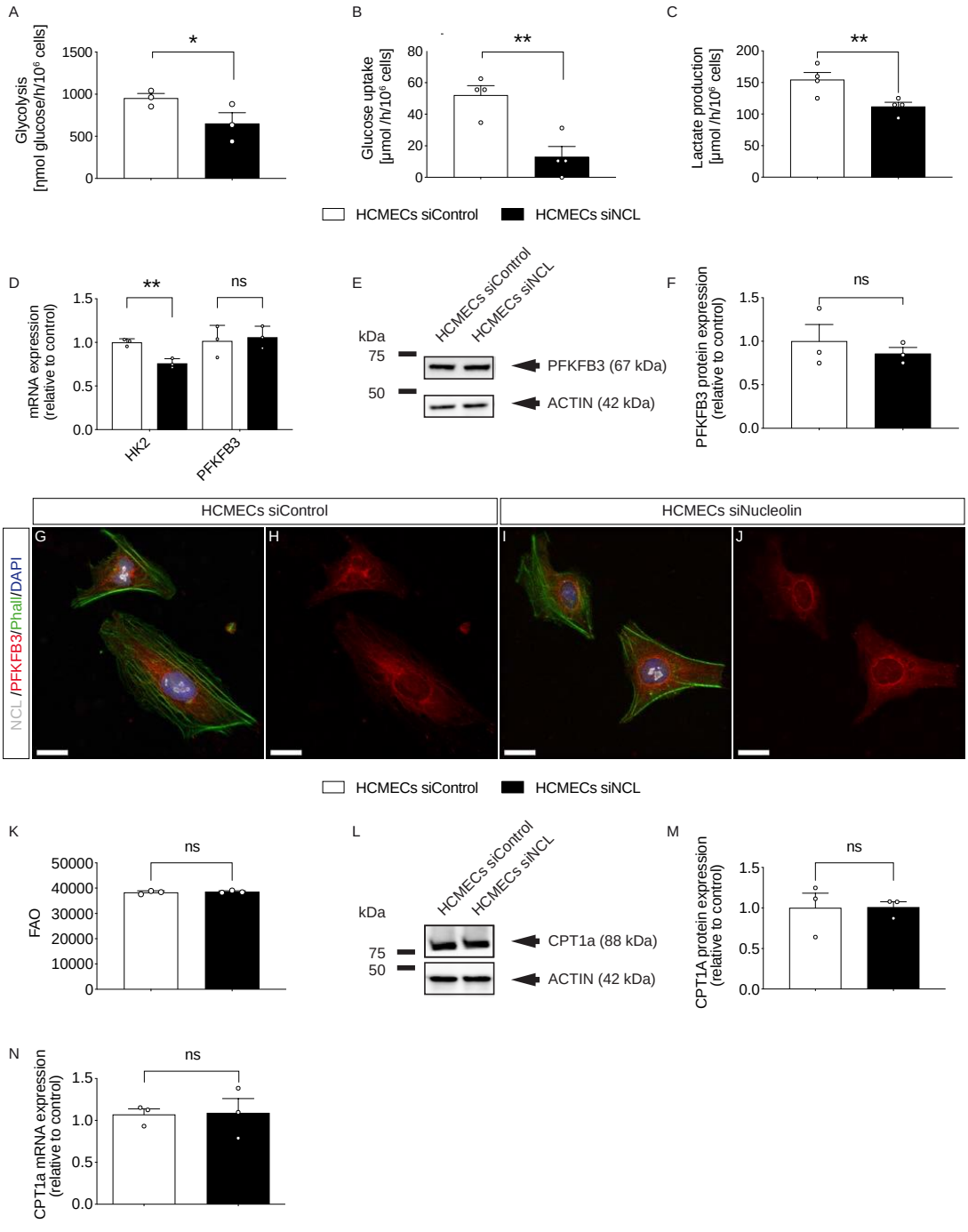
A
Glycolysis [ηmol glucose/h/10⁶ cells]
1500
1000
500
0
*
B
Glucose uptake [µmol /h/10⁶ cells]
80
60
40
20
0
**
C
Lactate production [µmol /h/10⁶ cells]
200
150
100
50
0
**
HCMECs siControl
HCMECs siNCL
D
mRNA expression (relative to control)
1.5
1.0
0.5
0.0
**
ns
HK2
PFKFB3
E
HCMECs siControl
HCMECs siNCL
kDa
75
50
PFKFB3 (67 kDa)
ACTIN (42 kDa)
F
PFKFB3 protein expression (relative to control)
1.5
1.0
0.5
0.0
ns
HCMECs siControl
HCMECs siNucleolin
NCL /PFKFB3/Phall/DAPI
G
H
I
J
HCMECs siControl
HCMECs siNCL
K
FAO
50000
40000
30000
20000
10000
0
ns
L
HCMECs siControl
HCMECs siNCL
kDa
75
50
CPT1a (88 kDa)
ACTIN (42 kDa)
M
CPT1A protein expression (relative to control)
1.5
1.0
0.5
0.0
ns
N
CPT1a mRNA expression (relative to control)
1.5
1.0
0.5
0.0
ns

Figure 10: Nucleolin positively regulates endothelial glucose metabolism via glycolytic enzymes including HK2 but does not affect fatty acid oxidation in human brain endothelial cells

A-**C** Metabolic assays of HCMECs, upon Nucleolin downregulation with small interfering RNA targeting Nucleolin. Nucleolin knockdown decreased the glycolytic flux (**A**, n=3), glucose uptake (**B**, n=4) and lactate production (**C**, n=4) in HCMECs as compared to the tested controls.

D Quantitative RT-PCR revealing a significant downregulation of about 30% of Hexokinase-2 (*HK2*) mRNA expression by siRNA-targeted Nucleolin knock down. 6-phosphofructo-2-kinase/fructose-2,6-biphosphatase 3 (*PFKFB3*) expression showed slight but no significant increase (n=3).

E-**F** Western blot using antibodies against PFKFB3 revealed no significant regulation of PFKFB3 expression by Nucleolin knock down (n=3).

G-**J** HCMECs were stained for Nucleolin (green), PFKFB3 (red), and the general nuclear marker DAPI (blue). No difference in PFKFB3 expression could be seen between Nucleolin knock down HCMECs (**G**,**H**) and the HCMECs treated with a control siRNA (**I**,**J**).

K Nucleolin knock down in HCMECs did not affect fatty acid oxidation (n=3).

L,**M** Western blot using antibodies against carnitine palmitoyltransferase 1A (CPT1a) showed no difference in CPT1a protein expression between Nucleolin knock-down HCMECs and the control condition (n=3).

N Quantitative RT-PCR showed no significant regulation of *CPT1A* mRNA expression upon siRNA-targeted Nucleolin knock down (n=3).

Data represent mean ± SEM. For statistical analysis, two-tailed unpaired Student's t -test were performed. **P* < 0.05, ***P* < 0.01. Scale bars: 20 μm in **G**-**J**